

Recasting Bounds on Long-lived Heavy Neutral Leptons in Terms of a Light Supersymmetric R-parity Violating Neutralino

Herbi K. Dreiner,^a Dominik Köhler,^a Saurabh Nangia,^a Martin Schürmann,^a and Zeren Simon Wang^{b,c}

^a*Bethe Center for Theoretical Physics & Physikalisches Institut der Universität Bonn, Nußallee 12, 53115 Bonn, Germany*

^b*Department of Physics, National Tsing Hua University, Hsinchu 300, Taiwan*

^c*Center for Theory and Computation, National Tsing Hua University, Hsinchu 300, Taiwan*

E-mail: dreiner@uni-bonn.de, koehler@physik.uni-bonn.de,
nangia@physik.uni-bonn.de, marschu@uni-bonn.de, wzs@mx.nthu.edu.tw

ABSTRACT: In R-parity-violating (RPV) supersymmetric models, light neutralinos with masses from the GeV-scale down to even zero are still allowed by all laboratory constraints. They are further consistent with dark matter observations, as they decay via RPV couplings. These RPV couplings are in general constrained to be small. Hence, such light neutralinos, if produced, *e.g.*, at a beam-dump or collider experiment, appear as displaced vertices or missing energy at the detector level. The same signatures have been extensively searched for at various experiments in the theoretical context of sterile neutrinos which mix with active neutrinos. In this work, we recast the sensitivity of both past and present experiments to sterile neutrinos to obtain new bounds on RPV couplings associated with a light neutralino. We find experiments such as T2K, BEBC, FASER, DUNE, and MoEDAL-MAPP can improve the current bounds on RPV couplings by up to 3 – 4 orders of magnitude in several benchmark scenarios.

Contents

1	Introduction	2
2	Model basics	4
2.1	RPV-MSSM with a light bino	4
2.1.1	Neutralino production and decay via $LL\bar{E}$ operators	4
2.1.2	Neutralino production and decay via $LQ\bar{D}$ operators	5
2.2	Heavy neutral leptons	5
2.3	The phenomenology connecting the light bino LSP and the HNL	6
3	Experiments and recasting	7
3.1	Direct-decay searches	7
3.1.1	Peak searches	7
3.1.2	Branching-ratio searches	9
3.2	Displaced-vertex searches	9
3.2.1	Beam-dump search	10
3.2.2	Collider searches	11
3.3	Missing-energy searches	12
3.4	Other searches	12
3.5	The recasting procedure	12
4	Numerical results	15
4.1	One-coupling scenarios	15
4.1.1	Bilinear scenarios	15
4.1.2	$LQ\bar{D}$ scenarios	16
4.1.3	$LL\bar{E}$ scenarios	20
4.2	Two-coupling scenarios	20
4.2.1	Pion scenarios	22
4.2.2	Kaon scenarios	24
4.2.3	D , D_s , and τ scenarios	27
4.2.4	B and B_c scenarios	28
5	Conclusions	31
A	Explicit neutralino production/decay widths with $LL\bar{E}$ operators	32

1 Introduction

With the discovery of a Standard-Model (SM)-like Higgs boson at the LHC in 2012 [1, 2], the SM is complete. Yet many questions beyond the Standard Model (BSM) remain. One avenue of exploration which has received considerable attention is new light, feebly interacting particles [3–12]. Such exotic states are predicted in many BSM theories and are often long-lived. Theoretical candidates for such long-lived particles (LLPs) range from heavy neutral leptons (HNLs), axion-like particles, dark scalars, and dark photons, to electroweakinos in variations of supersymmetric models, inelastic dark matter (DM), and many more. See, *e.g.*, Refs. [8, 13–15] for reviews on LLPs. They are usually motivated as explanations of either the non-vanishing active neutrino masses or of dark matter and could have a spin of $0, \frac{1}{2}, 1, \dots$, and a mass usually ranging from the sub-MeV scale up to the multi-TeV scale.

As an example, the HNLs (labeled as N in this work) are proposed hypothetical spin-half fermions that are SM-singlets which mix with the light active neutrinos. For certain mass values, they can explain simultaneously the neutrino masses, the observed dark matter, as well as the baryon asymmetry of the Universe [16]. They can give light neutrinos Dirac masses via the Yukawa term LHN in the Lagrangian with L and H being the lepton and Higgs doublets. This implies unnaturally small Yukawa couplings given the tiny neutrino masses [17–19]. One can also write down a Majorana mass term in the Lagrangian, leading to light Majorana neutrinos via the seesaw mechanisms [20–24]. While the vanilla type-I seesaw mechanism demands the mixing parameters should be small for the tiny active neutrino masses, larger values of mixing are legitimately conceived in other variations such as the linear seesaw model [25–27] and inverse seesaw model [28, 29]. Therefore, in phenomenological studies, the HNL mass and the mixing angles with the SM neutrinos are often assumed to be independent parameters.

Via mixing with the active neutrinos, the HNLs can participate in both charged-current and neutral-current interactions, coupled to both gauge bosons directly and the Higgs boson indirectly. They can thus be produced from decays of these bosons or from mesons, or through direct production at colliders. The HNL can decay leptonically or semi-leptonically, leading to a variety of signatures at the different experimental facilities. In particular, GeV-scale HNLs have received substantial attention in recent years, for they could originate from rare decays of mesons, which are copiously produced, *e.g.*, at beam-dump experiments, B -factories, and high-energy hadron colliders. Given the strict experimental upper bounds on the mixing of the HNLs and the active neutrinos, the more recent focus has been on small mixing angles, for which the GeV-scale HNLs are usually long-lived. Searches for these long-lived HNLs have been performed via many different signatures, including searches for missing energy, peak searches, as well as searches for displaced vertices (DV). See, *e.g.*, Refs. [30, 31] for summaries of these searches. Moreover, one could use the uncertainty on the measurements of the invisible decay width of mesons to put upper bounds on the long-lived HNLs, which contribute to the invisible decay width.

Besides the HNLs, supersymmetric electroweakinos, including charginos and neutralinos, are often considered as LLP candidates. See for instance Refs. [32, 33]. In particular, a

specific type of light neutralino in the GeV mass scale is still allowed by all observational and experimental constraints [34–45]; they are necessarily bino-like [34, 37] and have to decay to avoid overclosing the Universe [46–48]. One possibility is to consider R-parity-violating supersymmetry (RPV-SUSY) (see Refs. [49–51] for reviews), where the light binos decay via small but non-vanishing RPV couplings (see Ref. [52] for a detailed study of light bino decays). The minimal version is known as the R-parity-violating Minimal Supersymmetric Standard Model (RPV-MSSM) [53]. The RPV-MSSM solves the SM hierarchy problem as in the MSSM, and also predicts a very rich phenomenology at colliders [54–57]. *A priori* it is unknown if R-parity is conserved or broken, SUSY models with R-parity conservation or violation are equally legitimate, *e.g.*, see Refs. [58, 59]. Moreover, the RPV-MSSM can explain several experimental anomalies reported in recent years including the B -meson anomalies [60–64], the ANITA anomaly [65, 66], as well as the anomalous magnetic moment of the muon [62–64]. If R-parity is broken, one can write down operators which violate baryon- or lepton-number. Allowing all these operators to be non-vanishing would lead to a too fast proton decay rate, in conflict with the current experimental measurements [67, 68], unless all their couplings are extremely small. Therefore, we assume the discrete anomaly-free baryon triality symmetry B_3 [69–71], so that baryon-number is conserved. In this work, we restrict ourselves to the lepton-number-violating terms only. Further, the light bino is the lightest supersymmetric particle (LSP) in our study and decays only into SM particles via RPV couplings.

Via the lepton-number-violating RPV operators, the light bino decays lead to very similar final states as the NHL decays. Moreover, the corresponding RPV couplings are all bounded to be small by various low-energy observables and collider searches [50, 72–75]. The GeV-scale binos are hence expected to be long-lived, too, resulting in signatures such as missing energy and displaced vertices at various experiments. These similarities raise the question: is it possible to recast the extensive exclusion bounds on the HNLs in the literature into corresponding bounds on the light binos in the RPV-SUSY? In this work, we answer this question positively, by compiling a list of bounds on long-lived HNLs obtained in searches for all types of signatures mentioned above and recasting them into exclusion limits on the RPV-SUSY couplings as functions of the light bino mass for a selected list of benchmark scenarios.¹ We focus on exclusion bounds acquired in past experiments, as well as predicted search sensitivities for experiments that are ongoing or under construction. For future (and not yet approved) experiments, we consider only MoEDAL-MAPP2 [76, 77] and FASER2 [78] with 300 and 3000 fb^{−1} integrated luminosity, respectively, as they would be the successors of some ongoing experiments at the LHC, while the other future concepts such as MATHUSLA [14, 79, 80], and ANUBIS [81] are independent ones and are hence not studied here. We do not consider the approved experiment Hyper-Kamiokande [82, 83] for there is no available HNL-search sensitivity prediction that can be used with our recasting methods.

In the following section, we give the model basics of light binos in the RPV-SUSY and

¹Recently during the completion of this work, Ref. [31] appeared on arXiv; it employed similar strategies to recast the bounds on the HNLs in the minimal scenarios into those on the HNLs in effective field theories.

of the HNLs that mix with active neutrinos. The considered experiments are introduced in Sec 3, along with an explanation of our recasting procedure. We then present our numerical results for some representative benchmark scenarios in Sec. 4. Finally, in Sec. 5 we conclude the paper with a summary.

2 Model basics

2.1 RPV-MSSM with a light bino

In the R-parity-violating MSSM, the usual MSSM superpotential is extended by the following terms [53, 84]:

$$W_{\text{RPV}} = \kappa_i L_i H_u + \frac{1}{2} \lambda_{ijk} L_i L_j \bar{E}_k + \lambda'_{ijk} L_i Q_j \bar{D}_k + \frac{1}{2} \lambda''_{ijk} \bar{U}_i \bar{D}_j \bar{D}_k, \quad (2.1)$$

where L_i , \bar{E}_i , Q_i , \bar{U}_i , and \bar{D}_i are chiral superfields with generation indices $i, j, k \in \{1, 2, 3\}$ and H_u is one of the MSSM Higgs superfields. The λ_{ijk} , λ'_{ijk} (and λ''_{ijk}) are dimensionless Yukawa couplings, which imply lepton- (baryon-) number violating interactions and κ_i are dimensionful bilinear couplings violating lepton number. The Lagrangian in superfield-component form, as well as a complete list of RPV Feynman rules can be found, *e.g.*, in Appendix L of Ref. [85].

The RPV-MSSM allows for an unstable light long-lived neutralino, which we focus on here. A very light neutralino is necessarily dominantly bino-like [34] and a light bino currently avoids all experimental and astrophysical constraints even if it is massless [35, 41, 44]. In the following, we provide a concise overview of the production and decay of the lightest neutralino via $LL\bar{E}$ or $LQ\bar{D}$ operators. Moreover, for simplicity, we consider the lightest neutralino to be the LSP in this work. Note that we use the two-component fermion notation reviewed in Ref. [85].

2.1.1 Neutralino production and decay via $LL\bar{E}$ operators

For non-zero $LL\bar{E}$ couplings, neutralinos can be produced through charged lepton decays and can decay to lighter leptons. We provide the explicit general forms of the total decay widths for both the charged lepton and neutralino decays, employing the matrix element and necessary phase space integration in Appendix A. For all the relevant processes, we assume that all sfermions appear at the energy scale of the decaying particle as mass degenerate, *i.e.*, $m_{\tilde{f}} \simeq m_{\text{SUSY}} \gg m_{\tilde{\chi}_1^0}, m_{\ell^\pm}$. Further, the R-parity conserving neutralino gauge coupling is g' ($U(1)_Y$), since the neutralino is bino-like. As a result, we can write out the coefficients appearing in the matrix elements as, (*cf.* Appendix A)

$$c_{ijk} \simeq -\frac{\frac{1}{\sqrt{2}}\lambda_{ijk}g'}{m_{\text{SUSY}}^2} \quad \text{and} \quad k_{ijk} \simeq \frac{\sqrt{2}\lambda_{ijk}g'}{m_{\text{SUSY}}^2}. \quad (2.2)$$

Using Eq. (A.1), the relevant production widths can then be expressed as

$$\Gamma(\ell_k^\pm \rightarrow \tilde{\chi}_1^0 + \nu_i + \ell_j^\pm) = \Gamma_{LL\bar{E}}(\ell_k^\pm; \tilde{\chi}_1^0, \nu_i, \ell_j^\pm)[k_{ijk}, c_{ijk}, c_{ijk}], \quad (2.3)$$

$$\Gamma(\ell_k^\pm \rightarrow \tilde{\chi}_1^0 + \bar{\nu}_i + \ell_j^\pm) = \Gamma_{LL\bar{E}}(\ell_k^\pm; \tilde{\chi}_1^0, \bar{\nu}_i, \ell_j^\pm)[c_{ikj}, k_{ikj}, c_{ikj}]. \quad (2.4)$$

Similarly, the total widths of the subsequent neutralino decays $\tilde{\chi}_1^0 \rightarrow \bar{\nu}_i + \ell_j^- + \ell_k^+$ can be written as

$$\Gamma(\tilde{\chi}_1^0 \rightarrow \nu_i + \ell_j^- + \ell_k^+) = \Gamma_{LL\bar{E}}(\tilde{\chi}_1^0; \nu_i, \ell_j^-, \ell_k^+)[c_{ijk}, c_{ijk}, k_{ijk}], \quad (2.5)$$

$$\Gamma(\tilde{\chi}_1^0 \rightarrow \bar{\nu}_i + \ell_j^- + \ell_k^+) = \Gamma_{LL\bar{E}}(\tilde{\chi}_1^0; \bar{\nu}_i, \ell_j^-, \ell_k^+)[c_{ikj}, k_{ikj}, c_{ikj}]. \quad (2.6)$$

2.1.2 Neutralino production and decay via $LQ\bar{D}$ operators

Via the $LQ\bar{D}$ -operators mesons can decay into a bino accompanied by a lepton l_i . Subsequently, the bino decays via the same or another $LQ\bar{D}$ -operator to a lepton and two quarks, where the latter again hadronize into a meson (for a light enough bino). We consider charged mesons M_{ab}^+ with quark flavor content $(u_a \bar{d}_b)$ as well as neutral mesons M_{ab}^0 composed of $(d_a \bar{d}_b)$ and their charge conjugated equivalents. Neutral mesons composed of $(u_a \bar{u}_b)$ only contribute to higher multiplicity processes as $M \rightarrow \tilde{\chi}^0 + l_i + M'$, where M' denotes a lighter meson and l_i a charged lepton. We do *not* consider them here, since these are phase space suppressed by two to three orders of magnitude [86]. Both the bino production and decay width are therefore given by Ref. [86]:

$$\Gamma(M_{ab} \rightarrow \tilde{\chi}_1^0 + l_i) = \frac{\lambda^{\frac{1}{2}}(m_{M_{ab}}^2, m_{\tilde{\chi}_1^0}^2, m_{l_i}^2)}{64\pi m_{M_{ab}}^3} |G_{iab}^{S,f}|^2 (f_{M_{ab}}^S)^2 \left(m_{M_{ab}}^2 - m_{\tilde{\chi}_1^0}^2 - m_{l_i}^2 \right), \quad (2.7)$$

$$\Gamma(\tilde{\chi}_1^0 \rightarrow M_{ab} + l_i) = \frac{\lambda^{\frac{1}{2}}(m_{\tilde{\chi}_1^0}^2, m_{M_{ab}}^2, m_{l_i}^2)}{128\pi m_{\tilde{\chi}_1^0}^3} |G_{iab}^{S,f}|^2 (f_{M_{ab}}^S)^2 \left(m_{\tilde{\chi}_1^0}^2 + m_{l_i}^2 - m_{M_{ab}}^2 \right), \quad (2.8)$$

where $\lambda^{\frac{1}{2}}(x, y, z) = \sqrt{x^2 + y^2 + z^2 - 2xy - 2xz - 2yz}$ is the square root of the Källén function and $l_i = \ell_i^\pm$ or ν_i depending on the charge of M_{ab} . The coefficients $|G_{iab}^{S,f}|^2$ include the trilinear RPV couplings and are defined in Ref. [86], together with the meson scalar decay constants $f_{M_{ab}}^S$.

Furthermore, the $L_i L_j \bar{E}_j$ and $L_i Q_j \bar{D}_j$ operators additionally open the decay mode $\tilde{\chi}_1^0 \rightarrow (\gamma + \nu_i, \gamma + \bar{\nu}_i)$ at the one-loop level, *cf.* Ref. [87], but this signature is not considered in the present paper since to our knowledge the corresponding HNL-decay has to-date not been searched for.

Besides the displaced-vertex signature related to the decay channels computed above, it is possible that the lightest neutralino is so long-lived that it does not decay inside the considered detector and appears as missing energy.

2.2 Heavy neutral leptons

Heavy neutral leptons are a common feature of many SM extensions attempting to give an underlying explanation of the observed neutrino sector. The simplest HNL model one can implement is

$$\mathcal{L} \supset i\hat{N}_\alpha^\dagger \bar{\sigma}^\mu \partial_\mu \hat{N}^\alpha - \left[(Y_\nu)_\alpha^i \left(\Phi^0 \hat{\nu}_i \hat{N}^\alpha - \Phi^+ \ell_i \hat{N}^\alpha \right) + \frac{1}{2} M_\beta^\alpha \hat{N}_\alpha \hat{N}^\beta + \text{h.c.} \right], \quad (2.9)$$

where $i = 1, 2, 3$, Φ^+ and Φ^0 are the components of the SM $SU(2)_L$ Higgs doublet, and ℓ_i are the charged lepton mass eigenstates. Fields with a hat, $\hat{\nu}$ and \hat{N} , are the states before mass-diagonalizing the neutral lepton sector. $(Y_\nu)_\alpha^i$ are dimensionless Yukawa couplings and $M_\beta^\alpha = \text{diag}(M_{\hat{N}_1}, \dots)$ is a diagonal mass matrix. The index $\alpha = 1, 2, 3, \dots$ labels the (arbitrary many) HNLs in the theory. During electroweak symmetry breaking, the Higgs obtains a vacuum expectation value (vev) $v/\sqrt{2}$ with $v = 246$ GeV, which gives rise to mixing of the HNLs \hat{N}_α with active neutrinos $\hat{\nu}_i$, described by the mass matrix $M_{\nu N}$:

$$M_{\nu N} = \begin{pmatrix} \mathbb{0}_{3 \times 3} & M_D \\ M_D^T & M \end{pmatrix}. \quad (2.10)$$

Here, the off-diagonal entries are given by $(M_D)_\alpha^i = (Y_\nu)_\alpha^i v/\sqrt{2}$. The mass matrix can be perturbatively Takagi-block-diagonalized by introducing a unitary matrix U [85]. For simplicity, we assume there is only one kinematically relevant HNL in our study. In this case, the gauge eigenstate $\hat{\nu}_i$ receives first-order contributions from the mass eigenstate N , proportional to the following mixing matrix entry:

$$U_i \equiv U_4^i \equiv (Y_\nu^*)_1^i \frac{v}{\sqrt{2}M}. \quad (2.11)$$

The interaction Lagrangian with the neutrino mass eigenstates ν_i and N is then given by:

$$\mathcal{L} \supset -\frac{g}{\sqrt{2}} U_4^i W_\mu^- \ell_i^\dagger \bar{\sigma}^\mu N - \frac{g}{2c_W} U_4^i Z_\mu \nu_i^\dagger \bar{\sigma}^\mu N + \text{h.c.}, \quad (2.12)$$

where g is the $SU(2)_L$ gauge coupling and $c_W = \cos \theta_W$ is the cosine of the weak mixing angle.

2.3 The phenomenology connecting the light bino LSP and the HNL

The phenomenologies of the RPV-MSSM with a light bino $\tilde{\chi}_1^0$ and the SM extensions with one relevant HNL turn out to be very similar. This is not surprising, as the HNL and the bino have the same gauge quantum numbers after electroweak symmetry breaking. Currently existing bounds in the HNL parameter space spanned by (m_N, U_4^i) can thus be translated into bounds in the light-bino-RPV parameter space $(m_{\tilde{\chi}_1^0}, \lambda/m_{\text{SUSY}}^2)$, where λ labels here any appropriate $LL\bar{E}$ or $LQ\bar{D}$ coupling.

An additional analogy between the theories can be constructed by considering the bilinear RPV couplings κ_i [88], see Eq. (2.1). After integrating out the heavy higgsinos in the neutral fermion sector of the RPV-MSSM, one obtains a tree-level mixing of neutrinos with the bino, which is of the form

$$\mathcal{L} \supset \frac{g'}{2} \left(v_i - \frac{v_d \kappa_i}{\kappa^0} \right) \hat{\nu}_i \tilde{\chi}_1^0 + \text{h.c.}, \quad (2.13)$$

where v_i and v_d are the vevs of the sneutrinos and the MSSM Higgs H_d , respectively. κ^0 is the Higgsino mass parameter and g' the $U(1)_Y$ gauge coupling. This mixing can be interpreted as the off-diagonal entries in the neutral lepton mass matrix given in Eq. (2.10),

such that the elements of the matrix U , *cf.* Eqs. (2.11) and (2.12), can be mapped to the neutralino-neutrino mixing considered here:

$$U_4^i = \frac{g'}{2m_{\tilde{\chi}_1^0}} \left(v_i - \frac{v_d \kappa_i}{\kappa^0} \right). \quad (2.14)$$

For phenomenological computations, the Lagrangian given in Eq. (2.12) can be used, which would correspond to the trivial replacement

$$\hat{\nu} \text{ --- } \times \text{ --- } N \quad \longleftrightarrow \quad \hat{\nu} \text{ --- } \times \text{ --- } \tilde{\chi}_1^0 \quad (2.15)$$

where the inserted crosses denote the mixing. Thus, current HNL exclusion limits can be directly translated into bounds on the mixing strength in Eq. (2.13).

3 Experiments and recasting

In this section, we present the details of existing HNL searches and classify them according to their search strategy. We consider experiments employing the signatures: (i) direct decays, (ii) displaced vertices, and (iii) missing energy. For the direct-decay searches, we further partition our analysis into: (i.a) peak searches and (i.b) branching ratio searches. The displaced-vertices searches are also split further into: (ii.a) beam-dump searches and (ii.b) collider searches. Missing-energy searches allow us to derive new and stronger constraints on single RPV couplings. In addition, we present selected benchmark scenarios for which we will obtain single-coupling and coupling-product bounds within the RPV-MSSM framework. We provide an overview of the experiments, discussed in this section, in Table 1.

3.1 Direct-decay searches

One of the main ways to produce light HNLs is via the decay of light mesons such as pions and kaons. In direct searches, a beam of charged mesons is brought to a stop inside a scintillator where the mesons decay at rest, or the beam mesons are tagged and their positions, momenta, and timing information are measured by a silicon pixel spectrometer.

The energy spectrum of the visible secondary particle, *i.e.*, a muon or an electron, arising from these meson decays is measured. The signal shape of the energy spectrum can be compared with Monte-Carlo simulations for different HNL mass hypotheses. Finding no extra peaks in the secondary energy spectrum or rejecting each mass hypothesis allows us to exclude the relevant HNL parameters.

3.1.1 Peak searches

In peak searches, the energy spectrum of the secondary particle is scanned for additional peaks hinting at HNLs.

- At the Swiss Institute for Nuclear Research (SIN), a pion beam was used to put bounds on the mixing $|U_\mu|^2$ in the HNL mass range of 1-16 MeV [91].

Search Strategy	Ref.	Experiment	Status	HNL Mixing	HNL Mass region
Peak	[89]	PIENU	curr.	$ U_e $	65-153 MeV
	[90]	PIONEER	proj.	$ U_\mu $	15.7-33.8 MeV
	[90]	PIONEER	proj.	$ U_e $	65-135 MeV
	[91]	SIN	curr.	$ U_\mu $	1-16 MeV
	[92]	NA62	curr.	$ U_\mu $	144-462 MeV
	[93]	NA62	curr.	$ U_e $	200-384 MeV
	[94]	KEK	curr.	$ U_\mu $	160-230 MeV
	[95]	KEK	curr.	$ U_\mu $	70-300 MeV
Branching Ratio	[89]	PIENU	curr.	$ U_e $	0-65 MeV
	[90]	PIONEER	proj.	$ U_e $	0-65 MeV
Beam-dump	[96]	DUNE	proj.	$ U_e , U_\mu , U_\tau $	0-1968.34 MeV
	[97]	T2K	curr.	$ U_e , U_\mu $	10-490 MeV
	[98, 99]	CHARM	curr.	$ U_e , U_\mu $	300-1869.65 MeV
	[100]	CHARM	curr.	$ U_\tau $	290-1600 MeV
	[101]	NuTeV	curr.	$ U_\mu $	259-2000 MeV
	[102]	MicroBooNE	curr.	$ U_\mu $	20-200 MeV
	[103]	BEBC	curr.	$ U_e , U_\mu $	500-1750 MeV
	[104]	BEBC	curr.	$ U_\tau $	100-1650 MeV
	[105]	SK	curr.	$ U_e , U_\mu $	150-400 MeV
Collider	[106]	FASER	proj.	$ U_e , U_\mu , U_\tau $	0-6274.9 MeV
	[107]	MoEDAL-MAPP1	proj.	$ U_e $	0-6274.9 MeV
	[108]	BaBar	curr.	$ U_\tau $	100-1360 MeV
Missing Energy	[109]	NA62	curr.	$\text{BR}(\pi^0 \rightarrow \text{inv.})$	0-134.97 MeV
	[110]	BaBar	curr.	$\text{BR}(B^0 \rightarrow \text{inv.})$	0-5279.65 MeV

Table 1: Summary of experiments reviewed in Sec. 3, sorted by search strategy. We list the relevant references, the status of derived bounds (current or projected), the relevant HNL mixing, and the experimentally accessible HNL mass range.

- A search for massive neutrinos at the PIENU experiment [89] has been made in the decay of pions into positrons. No evidence was found for additional peaks in the positron energy spectrum. Thus, upper limits at 90% confidence level (CL) on $|U_e|^2$ were derived in the HNL mass region 60-135 MeV. In another analysis of the PIENU experiment [111], heavy neutrinos were searched for in pion decays into muons. The energy spectrum did not show any additional peaks other than the expected peak for a light neutrino. Thus, the analysis derived a bound on $|U_\mu|^2$ for the HNL mass range of 15.7-33.8 MeV.
- The PIONEER [90] experiment is a next-generation rare pion decay experiment. The experiment will perform the same search strategy as the PIENU experiment with higher statistics and significantly suppressed background. A peak search in the positron spectrum will allow probing $|U_e|^2$ in the HNL mass region 65-135 MeV. Further, a

search for an additional peak within the muon energy spectrum will allow us to test $|U_\mu|^2$ for $15.7 \text{ MeV} < m_N < 33.8 \text{ MeV}$.

- KEK [94] derived an upper bound on $|U_\mu|^2$ for a massive HNL in the mass range of 160-230 MeV. A similar search at KEK [95] led to an upper bound on $|U_\mu|^2$ in the HNL mass range of 70-300 MeV.
- Using a kaon beam, the NA62 collaboration placed bounds on $|U_e|^2$ for an HNL with a mass of 144-462 MeV [92]. The analysis approach is different from PIENU. In this case, a peak-search procedure measures the $K^+ \rightarrow e^+ N$ decay rate with respect to the $K^+ \rightarrow e^+ \nu$ rate for an assumed HNL mass m_N . The HNL mass is varied over the mentioned mass range. The benefit of this approach is the cancellations of residual detector inefficiencies, as well as trigger inefficiencies, and random veto losses. A similar analysis [93] has been performed to measure $|U_\mu|^2$ within the HNL mass range of 200-384 MeV. Note that both bounds of NA62 are derived with the assumption that the lifetime of the neutral particle exceeds 50 ns.
- The BaBar experiment [108] at SLAC has performed a search for the rare decay $\tau^- \rightarrow \pi^- \pi^- \pi^+ + N$ in the mass region of $100 < m_N < 1360 \text{ MeV}$. The observed kinematic phase space distribution of the hadronic system allows BaBar to place a stringent bound on $|U_\tau|^2$. However, the search is based on three-prong tau events. Technically, this allows us to derive a single coupling bound on λ'_{311} . However, the four-body production mode of the light neutralino would need proper phase-space consideration. Therefore, we do not include a reinterpretation of this search in our work and shall discuss it elsewhere.

3.1.2 Branching-ratio searches

It is possible to measure branching ratios of different pion decay modes. The ratio

$$R_{e/\mu} = \frac{\Gamma(\pi^+ \rightarrow e^+ + \nu(\gamma))}{\Gamma(\pi^+ \rightarrow \mu^+ + \nu(\gamma))}, \quad (3.1)$$

can be used to derive limits on the mixing $|U_e|^2$ in the region $m_N < 65 \text{ MeV}$. This has been performed by PIENU [112] and is planned for PIONEER [90].

3.2 Displaced-vertex searches

Beam-dump and collider experiments can produce HNLs via the same processes that produce light neutrinos. A proton beam hitting a fixed target typically produces a large number of pions and kaons, and also heavier mesons. If kinematically allowed, the decay of the primary mesons can produce HNLs, which will propagate freely since they are long-lived and interact only feebly. The HNLs produced at beam-dump experiments are typically boosted in the forward direction, which further increases their decay length in the lab frame. Hence, only a fraction of the produced HNLs decay at the location of the detector. To reduce possible background events, the experiments usually have a system of veto detectors equipped

for both charged and neutral particles. The search strategy relies on the visibility of the HNL decay products inside the detector; we will discuss these later.

In the following, we present displaced-vertex searches at beam-dump and collider experiments separately.

3.2.1 Beam-dump search

- At DUNE [113], HNLs can be produced via pion-, kaon-, and D -meson-decays. Ref. [96] predicts constraints on HNLs by searching for their decay products inside the DUNE Near Detector. It is assumed that only the three-neutrino final state is not detectable. The search strategy allows to measure all three mixings $|U_e|^2$, $|U_\mu|^2$ and $|U_\tau|^2$ for an HNL mass range up to the mass of the D_s -meson. Note that in the analysis, a single mixing element is assumed to dominate over the other two at a time.
- The T2K experiment [97] follows the same approach but uses a kaon beam. Thus, they derive bounds on both $|U_e|^2$ and $|U_\mu|^2$ for $10 \text{ MeV} < m_N < 490 \text{ MeV}$.
- Heavy neutral leptons in the CHARM beam-dump experiment are produced from D and D_s -meson decays.² The former allows to set bounds on $|U_e|^2$, $|U_\mu|^2$ for an HNL mass of $300\text{--}1869.65 \text{ MeV}$ [98, 99], and the latter allows to probe $|U_\tau|^2$ for $290 \text{ MeV} < m_N < 1600 \text{ MeV}$ [100].
- A search for HNLs has been performed at the NuTeV experiment [101] at Fermilab. The data were examined for HNLs decaying into muonic final states to derive bounds on the mixing $|U_\mu|^2$ of HNLs in the $0.25\text{--}2.0 \text{ GeV}$ mass range. See also Ref. [3] which directly considers the NuTeV data in terms of a light neutralino.
- An analysis of current data from the MicroBooNE experiment [102] can constrain the parameters of HNLs, that mix predominantly with muon-flavored neutrinos, for HNL masses between $20\text{--}200 \text{ MeV}$.
- The BEBC experiment derived limits on the HNL-light neutrino mixing parameters from a search for decays of heavy neutrinos in a proton beam-dump experiment [103]. It derived bounds on $|U_e|^2$, $|U_\mu|^2$ for an HNL mass between 0.5 GeV and 1.75 GeV . A re-analysis [104, 114] has demonstrated that the BEBC detector was also able to place bounds on the $|U_\tau|^2$ mixing for HNL masses higher than the kaon mass. This re-analysis has taken into account several production and decay channels of HNLs.
- For Super-Kamiokande (SK), the largest contribution to HNL production is through the decay of mesons produced in the atmosphere via cosmic rays. A secondary contribution to the flux comes from the HNL production in neutral-current scattering of atmospheric neutrinos passing through the Earth. The total number of HNL decays inside the detector within a given time window results in an upper bound on the

²In this work, we use “ D -mesons” (“ B -mesons”) to label the D^\pm mesons (B^\pm mesons), while D_s and B_c mesons are separately discussed. We do not take into account D^0 or B_s mesons.

HNL mixing. This approach is different from the displaced-decay search limits from beam dumps and allows one to derive bounds on $|U_e|^2$ and $|U_\mu|^2$ in the minimal HNL scenarios for masses between 150-400 MeV [105].

3.2.2 Collider searches

HNLs can be also searched for in (semi-)leptonic decays of mesons produced at the LHC via a similar mechanism as in beam-dump experiments. At colliders, particle collisions produce an abundance of mesons, such as pions, kaons, D -mesons, and B -mesons, which can further decay into HNLs. Far detectors at the LHC are sensitive to decaying, light LLPs with a decay length comparable with their distance to the interaction point, *e.g.*, of $\mathcal{O}(1) - \mathcal{O}(100)$ m. HNLs decaying inside the detector can be identified by their decay products, except for the invisible three-neutrino final state. To ensure a low background environment, the experiments are proposed to be set far away from the primary proton-proton collision points and require shielding between the interaction points and the detectors.

Some of the new detectors at the LHC are already approved and currently running: **FASER** [115] and **MoEDAL-MAPP1** [76]. We include these running HNL searches in order to reinterpret their projected sensitivity. Their follow-up programs, **FASER2** [78] and **MoEDAL-MAPP2** [77], have been proposed for operation during the high-luminosity LHC phase, with an expected final integrated luminosity 3 ab^{-1} and 300 fb^{-1} respectively, and are taken into account in our numerical analysis, as well.

FASER(2) [106]³ is intended to detect long-lived particles decaying inside the detector volume. A sensitivity estimate, taking the detector geometry into account, leads to a specific reach in $|U_e|^2$, $|U_\mu|^2$, and $|U_\tau|^2$ for an HNL with a mass up to the mass of the B_c -meson. Similarly, **MoEDAL-MAPP1(2)** [107, 116] can probe the mixing $|U_e|^2$ for HNL being produced in decays of D - and B -mesons for the same mass range as **FASER(2)**.

In addition, other experimental proposals for LLP far detectors include **MATHUSLA** [14, 79, 80], **ANUBIS** [81], **CODEX-b** [117], and **FACET** [118]. None of these proposed detectors has been officially approved. We therefore do *not* include them in our reinterpretation strategy. We still want to emphasize the prospect of these experiments in the search for light long-lived particles. Sensitivity estimates, worked out in detail on the minimal HNL scenarios in Ref. [107], would also provide possible discovery potential for the discussed light neutralino scenarios, as worked out for example in Refs. [87, 119–121]. These potential future experiments all intend to look for various BSM signatures which include neutralino decays induced by all of the LH_u , $LL\bar{E}$, and $LQ\bar{D}$ operators.

³In principle, Ref. [78] employs the most updated geometrical setup of **FASER(2)**, but the results shown therein for the HNLs do not separate the contributions from D - and B -mesons. Therefore, we have chosen to reinterpret the results given in Ref. [106] for the HNLs from the heavy mesons' decays, which are only slightly different from those given in Ref. [78].

3.3 Missing-energy searches

The NA62 search [109] allows us to derive bounds on the branching ratio of pions decaying into an invisible final state. This is achieved by the reconstruction of the charged particles in the process $K^+ \rightarrow \pi^+ \pi^0$. The analysis relies on the tracking of the charged K^+ and π^+ and can probe π^0 decay to any invisible final state. NA62 reported a 90% CL upper limit on $\text{BR}(\pi^0 \rightarrow \text{inv.}) < 4.4 \times 10^{-9}$. The search can be recast to derive bounds on RPV couplings which also contribute to the invisible decays of the pion. It turns out that the obtained limits are weaker than the currently existing bounds [56, 72] and are, therefore, omitted.

The BaBar experiment has also searched for rare decays $B_0 \rightarrow \text{inv.}$ [110]. The search relies on the identification of the other neutral B -meson, as the ‘tag side’, and thus, can measure a purely invisible decay width of the B -meson. The upper limit at the 90% CL yields $\text{BR}(B_0 \rightarrow \text{inv.}) < 2.4 \times 10^{-5}$. We can recast this search into bounds on the production coupling of a light long-lived neutralino.

We could not find existing searches for invisible decays of the other uncharged mesons, *i.e.*, K_S , K_L , and B_s . To derive limits on the decay of these mesons into a neutralino we consider the uncertainty of the total decay width of the mesons. We assume all visible decay modes to be measured within the decay width. The resulting uncertainty can be extended to account for additional invisible decays and potential errors in measurements. Thus, we use the uncertainty to establish an upper limit on the branching ratio into invisible final states, if kinematically allowed. These could contain neutrinos, HNLs, or neutralinos. Assuming the latter saturates the width uncertainty, we derive bounds on the $LQ\bar{D}$ couplings. The measured uncertainties can be found in Ref. [68].

We could not find bounds from direct searches for massive HNLs in the leptonic decays $\mu^- \rightarrow e^- + \nu + N$ and $\tau^- \rightarrow e^-/\mu^- + \nu + N$. There are only searches for the muons and the τ leptons to decay to a lighter charged lepton plus active neutrinos or a photon [122]. Thus, the existing limits on the branching ratio cannot be generalized for a massive HNL owing to kinematic assumptions. In this case, we again rely on the uncertainty of the decay widths. This allows us to derive bounds on the $LL\bar{E}$ couplings. Again, the uncertainties of the decay width are taken from Ref. [68].

3.4 Other searches

For the bilinear coupling scenarios, we use the most relevant and up-to-date constraints on the HNLs existing in the literature, which are summarized in Ref. [31]. Therefore, we supplement the results from the previously discussed experiments with data from TRIUMF [123], PSI [91], Borexino [124, 125], and atmospheric neutrinos scattering in the Earth [126].

3.5 The recasting procedure

The procedures for recasting the HNL bounds into limits on RPV scenarios depend on the RPV couplings that are switched on, and the search strategy of the experiments; they fall

into one of the following three categories:

- The most straightforward case is for scenarios involving bilinear RPV couplings. As discussed in Sec. 2, these couplings lead to mixing between the neutralino and the neutrinos, *cf.* Eq. (2.13). Thus, we directly translate HNL exclusion limits in the mixing vs. mass plane into bounds in the RPV coupling vs. neutralino mass plane, using Eq. (2.14).
- In RPV scenarios involving $LQ\bar{D}$ or $LL\bar{E}$ operators, and a (detector-level) stable neutralino produced in the decay of a meson or lepton, missing-energy searches and peak searches can provide sensitivity. We use the HNL exclusion limits (typically in the mixing vs. mass plane) in order to determine the bounds on the decay width of the relevant meson/lepton into an HNL (see, for instance, Refs. [127, 128]). Since replacing the HNL with a light bino of the same mass does not change the experimental signature and the kinematics, we can simply equate the above with the corresponding decay width of the same meson/lepton into a bino in the RPV model, using the expressions given in Sec. 2; this gives us the bound on the relevant RPV coupling in terms of the bino mass.
- For RPV scenarios involving $LQ\bar{D}$ or $LL\bar{E}$ operators where the neutralino is produced in meson/lepton decays, and is *unstable* at the detector scales, displaced-vertex searches (beam dump or collider) can apply. In this case, we use the long-lifetime approximation to calculate the number of decay events reconstructed in the detector, following the arguments outlined in Ref. [116] (see also Ref. [31]); we review the procedure briefly now. Consider a beam-dump or collider experiment that searches for HNLs via displaced vertices. Let the HNL, N , be produced in the decay of a parent particle P (for instance, a pion).⁴ Then, the number of detected events for a final state, Y , produced in the decay of N can be estimated as,

$$N_{\text{events}}^{\text{HNL}} = N_P \times \text{BR}(P \rightarrow N + X) \times \text{BR}(N \rightarrow Y) \times \epsilon, \quad (3.2)$$

where N_P is the number of P produced at the experiment, X are any additional objects produced in P 's decay that are not of interest to us, and the BRs are the corresponding branching ratios. ϵ is a factor accounting for the detector acceptance and efficiency. This factor is linearly proportional to the probability for the HNL to decay inside the detector ($P[\text{decay}]$). It also depends on experiment-specific information such as the detector type and its geometry. In the limit of a long-lived HNL, such that the boosted decay length is much larger than the distance ΔL from the interaction point of the experiment to the first edge of the detector along the direction of travel of the HNL, to a good approximation we have [116],

$$P[\text{decay}] \approx \frac{\Delta L \times \Gamma_N}{\beta_N \gamma_N}, \quad (3.3)$$

⁴We are assuming that the direct production of the HNL (or bino) is suppressed compared to indirect production via decays of mesons and leptons, which is typically the case.

where Γ_N , β_N , and γ_N represent the total decay width, the relativistic velocity, and the Lorentz boost factor of the HNL, respectively. Inserting this in Eq. (3.2), we obtain,

$$N_{\text{events}}^{\text{HNL}} = A \times \frac{\text{BR}(P \rightarrow N + X) \times \Gamma(N \rightarrow Y)}{\beta_N \gamma_N}, \quad (3.4)$$

where all the quantities depending on the HNL model details are written explicitly, and the remaining experiment-specific factors of Eq. (3.4) have been absorbed into the proportionality factor A . Now, assume that there is also an RPV scenario in which the light bino, $\tilde{\chi}_1^0$, is produced in P decays, and has a decay mode into Y . Analogously, we can write,

$$N_{\text{events}}^{\text{RPV}} = A \times \frac{\text{BR}(P \rightarrow \tilde{\chi}_1^0 + X') \times \Gamma(\tilde{\chi}_1^0 \rightarrow Y)}{\beta_{\tilde{\chi}_1^0} \gamma_{\tilde{\chi}_1^0}}, \quad (3.5)$$

where the HNL is now replaced by the bino. Here, since both the light bino and the HNL are produced in the same meson's decay at the identical experiment, the proportionality factor A can be legitimately assumed to be essentially the same. Thus, combining the two equations, we obtain a simple scaling relation between the two models:

$$\frac{N_{\text{events}}^{\text{RPV}}}{N_{\text{events}}^{\text{HNL}}} = \frac{\text{BR}(P \rightarrow \tilde{\chi}_1^0 + X') \times \Gamma(\tilde{\chi}_1^0 \rightarrow Y) \times \beta_N \gamma_N}{\text{BR}(P \rightarrow N + X) \times \Gamma(N \rightarrow Y) \times \beta_{\tilde{\chi}_1^0} \gamma_{\tilde{\chi}_1^0}}. \quad (3.6)$$

For an HNL and a light bino with the same mass, we can further simplify the above expression in the limit where the HNL and the bino carry the same energy in the lab frame. In this case, the $\beta\gamma$ factors cancel out, and we have,

$$\frac{N_{\text{events}}^{\text{RPV}}}{N_{\text{events}}^{\text{HNL}}} = \frac{\text{BR}(P \rightarrow \tilde{\chi}_1^0 + X') \times \Gamma(\tilde{\chi}_1^0 \rightarrow Y)}{\text{BR}(P \rightarrow N + X) \times \Gamma(N \rightarrow Y)}, \quad (3.7)$$

which is completely free from any experiment-specific factors. This will be the master expression we use for recasting DV searches. We note that, technically, having different X and X' induces different kinematics for the HNL and the bino. For instance, the two final states could have different masses, or even contain differing number of objects, thus affecting the energy carried by the bino relative to the HNL. However, typically, the experiments we consider produce the parent particles (or their decay products) with significant boosts, in which case the above formula is only modified mildly. On the other hand, we stress that the HNL and the bino must be produced in the decay of the same (or similar) parents, and must decay into the same final state since these can significantly alter the detector acceptances and efficiencies.⁵

To use Eq. (3.7), assume that a given DV search for HNLs concludes without discovery, and obtains bounds on the HNL model parameters corresponding to a certain signal-event number, $[N_{\text{events}}^{\text{HNL}}]_{\text{bound}}$. Since the signal (and kinematics) in the RPV model is

⁵Actually, the final states into which the HNL and bino decay need not be identical, *e.g.*, the invisible objects contained in both do not need to match; the crucial part is that the detection efficiencies at the considered experiment must be the same.

the same, this bound also applies to the light binos: $[N_{\text{events}}^{\text{RPV}}]_{\text{bound}} = [N_{\text{events}}^{\text{HNL}}]_{\text{bound}}$. Plugging this into Eq. (3.7), we arrive at,

$$[\text{BR}(P \rightarrow \tilde{\chi}_1^0 + X') \times \Gamma(\tilde{\chi}_1^0 \rightarrow Y)]_{\text{bound}} = [\text{BR}(P \rightarrow N + X) \times \Gamma(N \rightarrow Y)]_{\text{bound}}. \quad (3.8)$$

The right-hand side of the above equation can be evaluated by using the bounds on the HNL mass and mixings as input (see, for instance, Refs. [127, 129, 130] for explicit expressions for all relevant decay widths in terms of these parameters), while the expressions for the RPV counterparts appear in Sec. 2 and depend on the RPV couplings, sfermion masses, as well as the neutralino mass.

4 Numerical results

In order to present our results, we consider benchmark scenarios with one or two non-vanishing RPV couplings. Additional non-zero RPV couplings could allow for further neutralino decay channels to open up; these would modify the relevant branching ratios and neutralino decay length, and hence, the presented sensitivity limits.

4.1 One-coupling scenarios

We first consider scenarios where only one non-zero RPV operator contributes to the relevant physical process at a time. For each of the RPV couplings in Eq. (2.1) (except the λ''_{ijk} 's), we list the relevant HNL searches providing constraints in Table 2. We now discuss the sensitivity limits for each category of RPV coupling in detail.

4.1.1 Bilinear scenarios

The bilinear couplings (κ^i and the sneutrino vacuum expectation values) induce a mixing between the light bino and the three light neutrinos, *cf.* Eq. (2.13). Thus, all HNL searches constraining the mixing between the HNL and the neutrinos directly imply constraints on these couplings. The exclusion limits are shown in Fig. 1. These have been read off from Ref. [31]. The bilinear couplings also generate mass terms for the neutrinos – see, for instance, Refs. [53, 84, 131–133] – leading to the constraint $v_i, \kappa^i \lesssim \mathcal{O}(1 \text{ MeV})$ [53]; this is depicted as a gray horizontal line in the plot.⁶ We find that the reinterpreted bounds from the HNL searches corresponding to the light-flavor neutrinos (e and μ) have sensitivity to regions beyond the current limits at low neutralino masses below 500 MeV. In this region, the most constraining limits come from PIENU [89, 111, 112], NA62 [92, 93], and T2K [97, 134]. Beyond this mass, and for the tau case – where charged kaon and pion decay into HNLs are kinematically forbidden – existing limits are weaker.

⁶We note that the existing limit comes from the cosmological bound on the neutrino masses, and is thus scenario-dependent [68]. Further, there is also dependence on undetermined supersymmetric parameters.

Coupling	Direct Decays	E_T^{miss}	DV	Label
κ^i	ν -mixing [31]	ν -mixing [31]	ν -mixing [31]	κ
λ'_{a11}	$\pi^\pm \rightarrow e_a^\pm + \tilde{\chi}_1^0$ [89, 90, 111, 112]	$\pi^0 \rightarrow \text{invis.}$ [109]	\times	λ'_π
λ'_{311}	$(\times) \tau^\pm \rightarrow \{\pi^\pm/\rho^\pm\} + \tilde{\chi}_1^0$	$\pi^0 \rightarrow \text{invis.}$ [109]	$\tau^\pm \rightarrow \pi^\pm + \tilde{\chi}_1^0; \tilde{\chi}_1^0 \rightarrow \nu_\tau + \{\pi^0/\rho^0/\eta/\eta'/\omega\}$ [96, 106, 107, 116]	
λ'_{a12}	$K^\pm \rightarrow e_a^\pm + \tilde{\chi}_1^0$ [92–95]	$K_L^0 \rightarrow \text{invis.}$ [68]	\times	λ'_K
λ'_{312}	$(\times) \tau^\pm \rightarrow K^\pm + \tilde{\chi}_1^0$	$K_L^0 \rightarrow \text{invis.}$ [68]	\times	
λ'_{i13}	$(\times) B^\pm \rightarrow e_i^\pm + \tilde{\chi}_1^0$	$B^0 \rightarrow \text{invis.}$ [110]	\times	λ'_{B1}
λ'_{i21}	$(\times) D^\pm \rightarrow e_i^\pm + \tilde{\chi}_1^0$	$K_L^0 \rightarrow \text{invis.}$ [68]	\times	$\lambda'_{D/K}$
λ'_{i22}	$(\times) D_s^\pm \rightarrow e_i^\pm + \tilde{\chi}_1^0$	\times	$D_s^\pm \rightarrow e_i^\pm + \tilde{\chi}_1^0; \tilde{\chi}_1^0 \rightarrow \nu_e + \{\phi/\eta/\eta'\}$ [96, 106, 107, 116]	λ'_{D_s}
λ'_{i23}	$(\times) B_c^\pm \rightarrow e_i^\pm + \tilde{\chi}_1^0$	$B_s^0 \rightarrow \text{invis.}$ [68]	\times	λ'_{B_c/B_s}
λ'_{i31}	\times	$B^0 \rightarrow \text{invis.}$ [110]	\times	λ'_{B2}
λ'_{i32}	\times	$B_s^0 \rightarrow \text{invis.}$ [68]	\times	λ'_{B_s}
λ'_{i33}	\times	\times	\times	—
λ_{12a}	\times	$\mu^\pm \rightarrow e^\pm + \text{invis.}$ [68]	\times	λ_μ
$\lambda_{123}; \lambda_{13i};$ $\lambda_{232}; \lambda_{233}$	\times	$\tau^\pm \rightarrow \{e^\pm/\mu^\pm\} + \text{invis.}$ [68]	\times	λ_τ
λ_{231}	\times	$\{\tau^\pm/\mu^\pm\} \rightarrow e^\pm + \text{invis.}$ [68]	\times	$\lambda_{\tau/\mu}$

Table 2: Details of the searches providing constraints when only one non-zero RPV operator contributes at a time. We list all the bilinear, $LQ\bar{D}$, and $LL\bar{E}$ operators in the first column (by coupling). The second to fourth columns contain the physical processes that provide constraints and the references to the relevant existing HNL searches targeting them. The fifth column indicates our labeling scheme for the scenarios. \times denotes the absence of a constraining process, while (\times) labels that, in principle, the listed process may provide constraints but we could not find a relevant existing HNL search. In the table, $a \in \{1, 2\}$ and $i \in \{1, 2, 3\}$.

4.1.2 $LQ\bar{D}$ scenarios

For the remaining one-coupling scenarios, all existing limits on the RPV couplings are taken from Ref. [56]. The $L_i Q_1 \bar{D}_1$ -operators couple to pions. With $i = 1$, the decay $\pi^\pm \rightarrow e^\pm + \tilde{\chi}_1^0$ is allowed, for masses $m_{\tilde{\chi}_1^0} \leq m_{\pi^\pm} - m_e$.⁷ This process has been searched for in the context of HNLs, and the most stringent existing limits are provided by PIENU [89]. Additionally, the approved PIONEER [90] experiment is projected to have sensitivity beyond these limits. We show the resulting contours in Fig. 2a. The sharp drop in sensitivity at $m_{\tilde{\chi}_1^0} \approx 65 \text{ MeV}$ occurs because branching ratio measurements provide bounds below this

⁷In the small region of phase space, $m_{\pi^0} + m_{\nu_e} < m_{\tilde{\chi}_1^0} < m_\pi^\pm - m_e$, $\lambda'_{111} \neq 0$ allows for the neutralino to decay into a neutrino and a pion; displaced-vertex searches can constrain this process. However, we have ignored this in Table 2 (also analogously for the kaon).

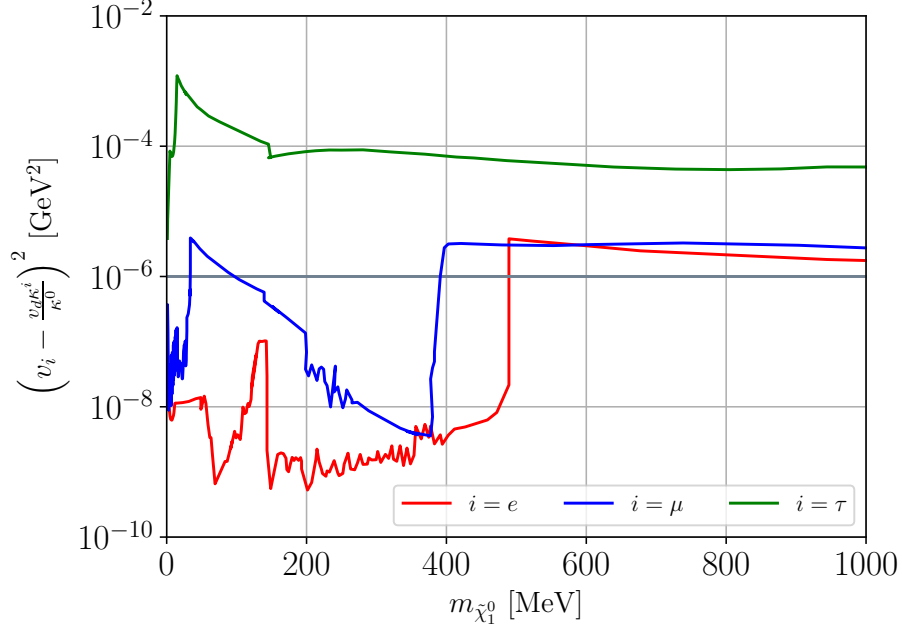


Figure 1: Exclusion limits on bilinear RPV couplings as a function of the light bino mass, reinterpreted from existing HNL searches. The current limit on the bilinear couplings is shown as a horizontal gray line.

mass, and peak searches above this threshold, *cf.* discussion in Sec. 3. Similarly, for $i = 2$, the pion can decay into a muon instead of an electron, in the mass range, $m_{\tilde{\chi}_1^0} \leq m_{\pi^\pm} - m_\mu$. This time, the sensitivity range, shown in Fig. 2b, comes from SIN [91] in addition to PIENU [111] and PIONEER. Finally, with $i = 3$, the decays, $\tau^\pm \rightarrow \pi^\pm(\rho^\pm) + \tilde{\chi}_1^0$, can occur if kinematically allowed. While we could not find a direct search for such a process involving an HNL, $\lambda'_{311} \neq 0$ additionally allows the neutralino to decay into a tau neutrino and one of $\pi^0/\rho^0/\eta/\eta'/\omega$. Thus, displaced-vertex searches at DUNE [96], FASER(2) [106] and MoEDAL-MAPP2 [107, 116] can show sensitivity.⁸ We present the corresponding combined projected sensitivity reach in Fig. 2c. In all the plots, we also show the best existing constraints on the RPV couplings for different sfermion masses. For λ'_{111} , this comes from neutrinoless double beta decay searches [73, 138], and is rather stringent compared to the other two couplings. Nevertheless, we see that the reinterpreted bounds easily outperform these existing constraints in the major part of the phase space region. We also note that in all of the above scenarios, the RPV couplings contribute to the invisible decay width of the pion, via the decay into a neutrino and the bino, given the long lifetime of the latter. However, the limits obtained this way are not competitive compared with the above ones.

Next, we consider the kaon scenarios, involving couplings of the type λ'_{i12} . For $i \in \{1, 2\}$, as for the pion case above, the decay mode into an electron or a muon along with the bino opens up for the kaon, below the relevant kinematic thresholds. The most constraining

⁸See also Ref. [135] for a proposed search at Belle II [136, 137] for a light bino with non-vanishing RPV couplings λ'_{311} or λ'_{312} .

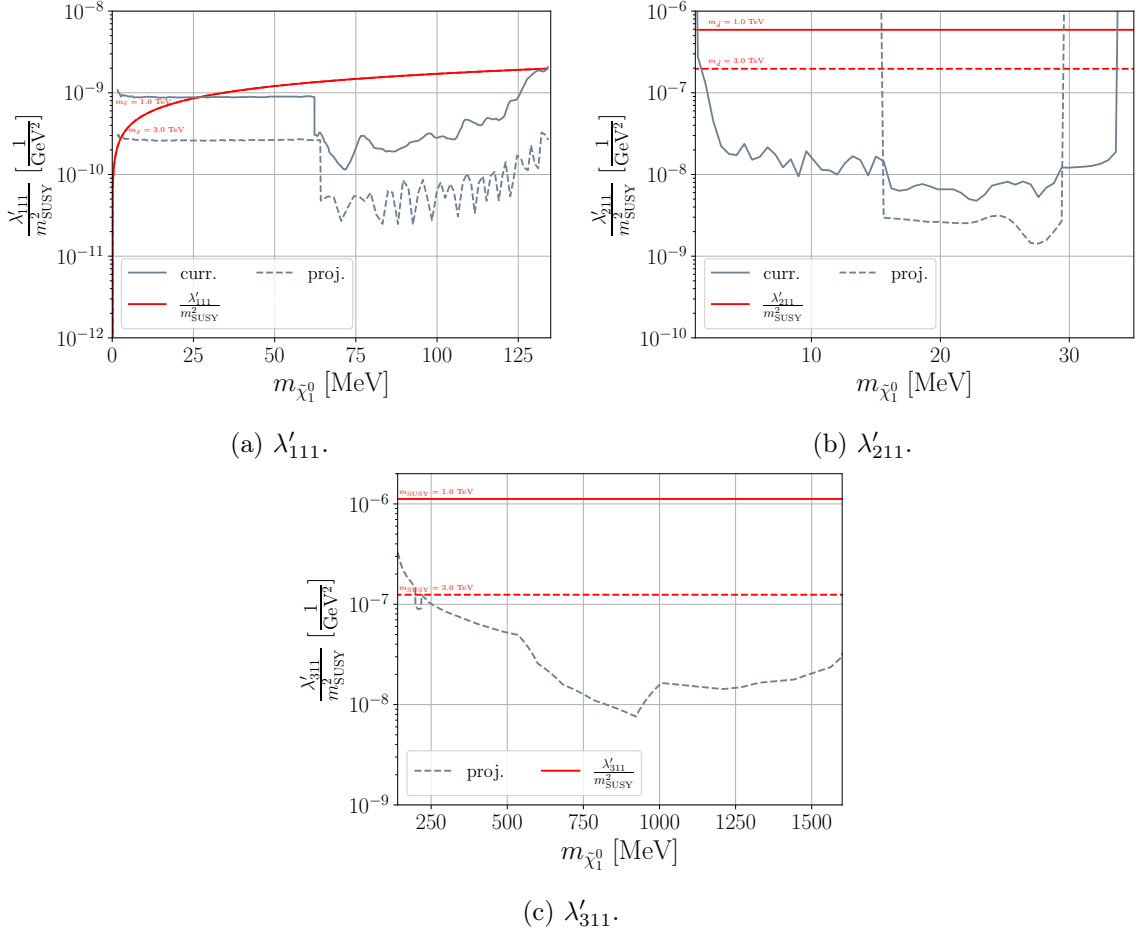


Figure 2: Sensitivity limits on the λ'_{π} one-coupling scenarios of Table 2 as a function of the light bino mass, reinterpreted from existing HNL searches. Current (projected) limits obtained from the reinterpretation are shown as solid (dashed) gray lines. The existing limits on the RPV couplings are also shown in red, with the solid and dashed lines corresponding to varying assumptions of unknown SUSY mass scales.

current limits come from KEK [94, 95] and NA62 [92, 93], and are depicted in Fig. 3a (electron case), and Fig. 3b (muon case). The degradation at $m_{\tilde{\chi}_1^0} \sim 200$ MeV in Fig. 3b occurs because the KEK-limit only applies up to this mass; beyond it the NA62 limit applies. Once again, both $L_i Q_1 \bar{D}_2$ also contribute to the invisible decays of the kaon but the resulting limits are weaker than those shown. However, for λ'_{312} – where we could not find an existing HNL direct search for the charged decay, $\tau^\pm \rightarrow K^\pm + \tilde{\chi}_1^0$ (see Footnote 8), the invisible width of K_L^0 can indeed be used to derive limits. Since there is no direct bound on this width, we use the uncertainty on the total measured width of K_L^0 [68] to estimate the upper bound, $\text{BR}(K_L^0 \rightarrow \text{invis.}) < 4.1 \times 10^{-3}$. This, then, can be used to constrain λ'_{312} since it induces the decay of K_L^0 into a neutrino and a bino. Analogously, the invisible width also provides limits on couplings of the type λ'_{i21} . Here also, we could not find existing direct searches for the relevant charged decay of D into a lepton and an HNL. All these

constraints are displayed in Fig. 3c. Once again, we can see that the reinterpreted bounds exclude regions of phase space orders of magnitude beyond those ruled out by the existing constraints on the RPV operators (also shown in the plots).

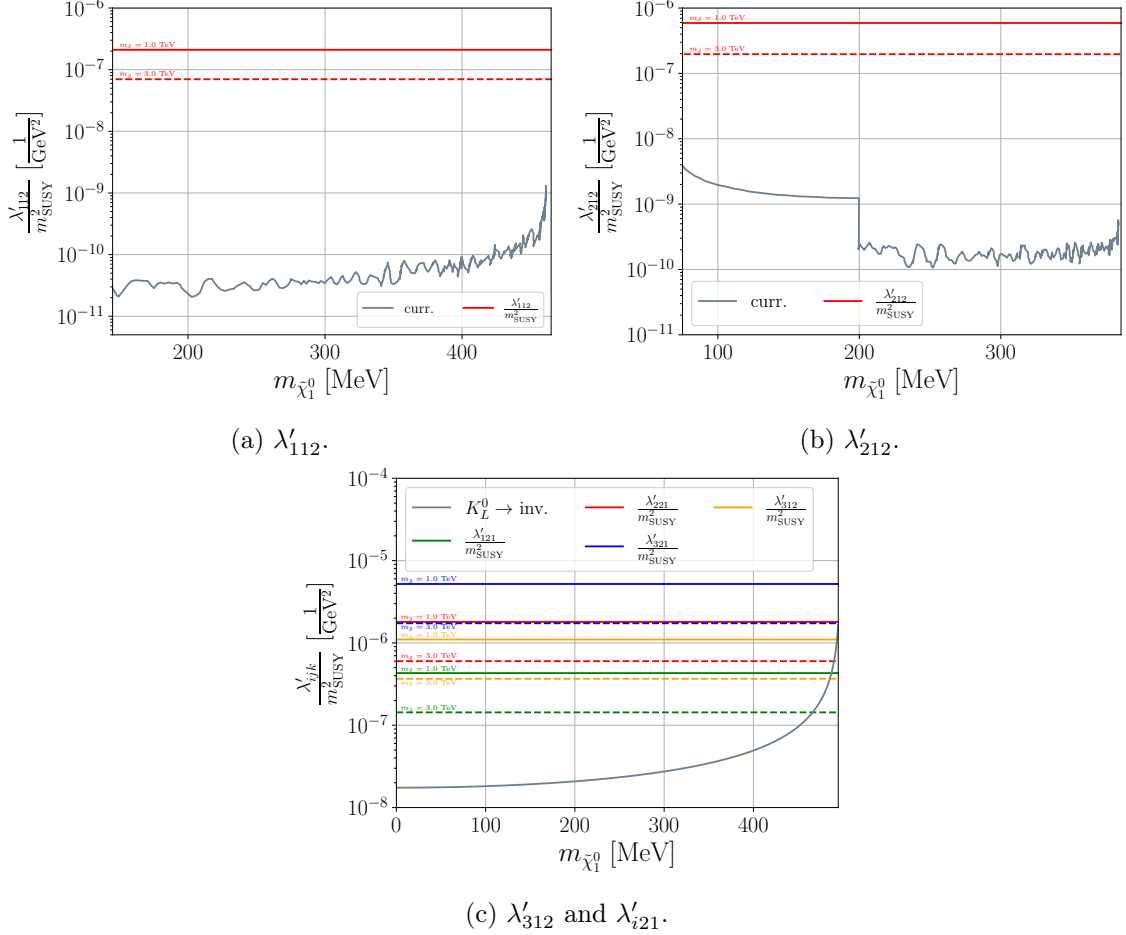


Figure 3: As in Fig. 2 but for the λ'_K and $\lambda'_{D/K}$ benchmarks of Table 2. The existing limits on the RPV couplings are shown in red, yellow, green, and blue.

Similarly, for couplings of the type λ'_{i13} and λ'_{i31} , we can use the invisible width of B^0 . Here, direct measurements at BaBar [110] provide the stringent constraint, $\text{BR}(B^0 \rightarrow \text{invis.}) < 2.4 \times 10^{-5}$. The resulting bounds are shown in Fig. 4.

For the couplings λ'_{a22} , with $a \in \{1, 2\}$, we use potential future displaced-vertex searches from DUNE [96], FASER2 [106], and MoEDAL-MAPP2 [107, 116] since we could not find a direct search for the decay of D_s^\pm into an HNL. In these scenarios, the neutralino decays via the RPV operator into a neutrino and one of $\phi/\eta/\eta'$. This implies the mass range, $548 \text{ MeV} \lesssim m_{\tilde{\chi}_1^0} < m_{D_s} - m_{e_a}$. Thus, the corresponding scenario with $\lambda'_{322} \neq 0$ involving a tau lepton is not possible. We show the resulting sensitivity limits in Fig. 5.

For the remaining $LQ\bar{D}$ operators, there are either no relevant processes providing constraints through meson or lepton decays ($\lambda'_{322}, \lambda'_{i33}$), or the obtained limits are not competitive with the existing bounds ($\lambda'_{i23}, \lambda'_{i32}$).

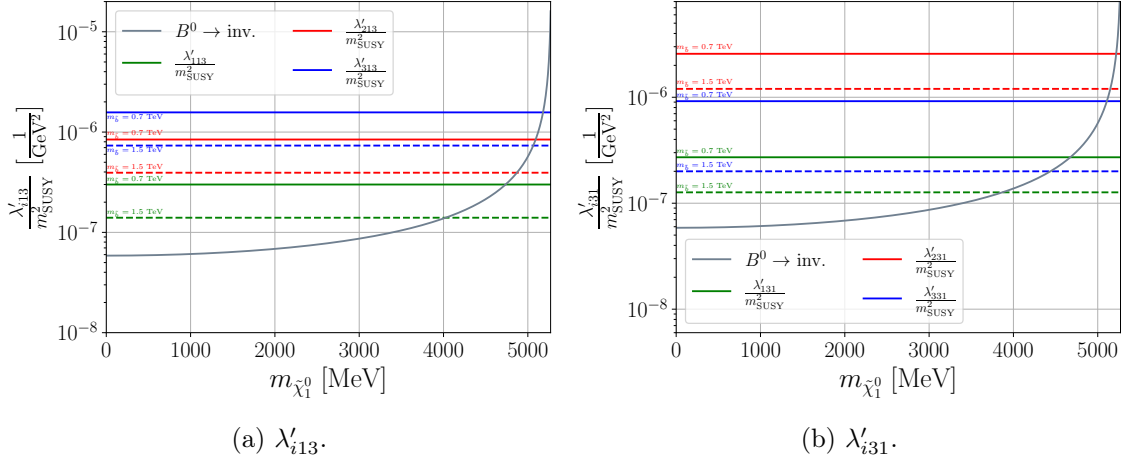


Figure 4: As in Fig. 2 but for the λ'_{B1} and λ'_{B2} benchmarks of Table 2. The existing limits on the RPV couplings are shown in red, green, and blue.

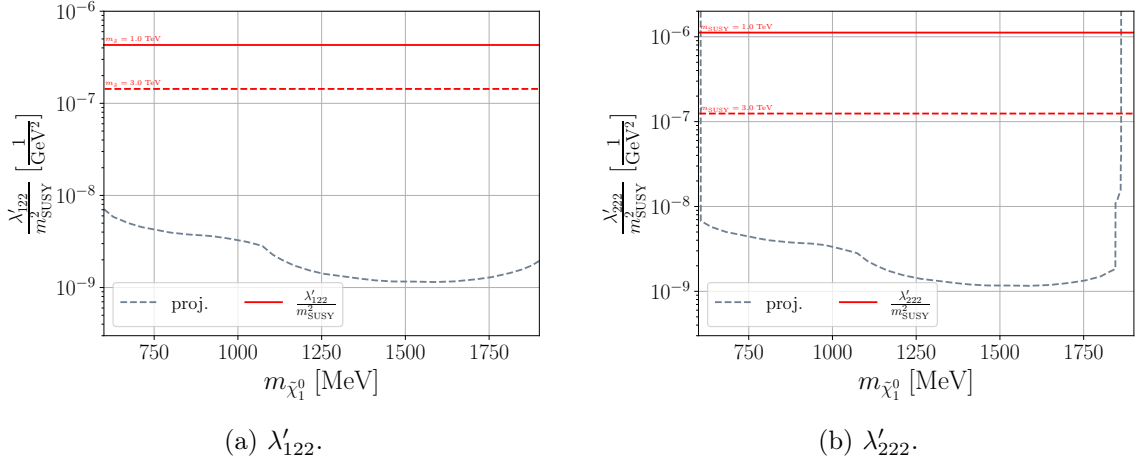


Figure 5: As in Fig. 2 but for the λ'_{D_s} benchmarks of Table 2.

4.1.3 $LL\bar{E}$ scenarios

For the λ_μ , λ_τ and $\lambda_{\tau/\mu}$ scenarios of Table 2, the corresponding operators contribute to the leptonic decays of the muon and the tau. Since we could not find direct measurements for the process $\mu^\pm \rightarrow e^\pm + \text{invis.}$ (and analogously for $\tau \rightarrow e$ and $\tau \rightarrow \mu$), where the invisible final state may be massive, we use the uncertainty on the muon decay width [68] to obtain an estimated bound, $\text{BR}(\mu^\pm \rightarrow e^\pm + \text{invis.}) < 1.0 \times 10^{-6}$. This leads to constraints on the λ_μ and $\lambda_{\tau/\mu}$ scenarios, as shown in Fig. 6. The analogous procedure with τ leads to limits weaker than the existing constraints and are hence not presented here.

4.2 Two-coupling scenarios

Next, we consider scenarios where two RPV operators are simultaneously switched on; one corresponds to the production of the bino LSP, while the other leads to the decay. We can

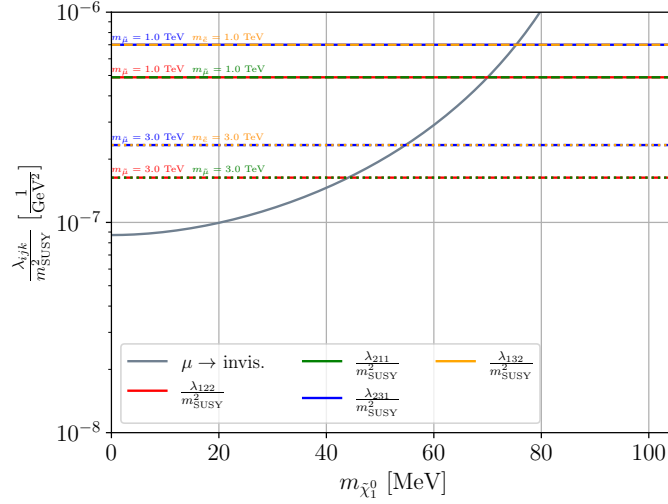


Figure 6: As in Fig. 2 but for the λ'_μ and $\lambda'_{\tau/\mu}$ benchmarks of Table 2. The existing limits on the RPV couplings are shown in red, yellow, green, and blue.

classify these scenarios based on the parent particle producing the neutralino; this then fixes the production RPV coupling. The relevant possibilities for the parent particles at beam-dump searches and colliders are: pions, kaons, D mesons, D_s mesons, B mesons, B_c mesons, and τ leptons.⁹ The corresponding production RPV couplings (and processes) can be read off from Table 2, *e.g.*, λ'_{a11} for the pion, etc.

The produced neutralino, owing to its long lifetime, then travels a certain macroscopic distance and decays via the other RPV coupling. Thus, displaced-vertex searches for HNLs are sensitive to such scenarios, if the final states match the decay products of the bino. We list, in Table 3, all relevant final states of such searches, along with the relevant kinematic thresholds at which the HNL can decay into them. Consulting the discussion in Sec. 2, we see that each of these final states can also arise from bino decays.

Channel	Threshold	Channel	Threshold
$\nu e^+ e^-$	1.02 MeV	$\mu^\mp K^\pm$	599 MeV
$\nu e^\pm \mu^\mp$	105 MeV	$\nu \rho^0$	776 MeV
$\nu \pi^0$	135 MeV	$e^\mp \rho^\pm$	776 MeV
$e^\mp \pi^\pm$	140 MeV	$\nu \omega$	783 MeV
$\nu \mu^+ \mu^-$	210 MeV	$\mu^\mp \rho^\pm$	882 MeV
$\mu^\mp \pi^\pm$	245 MeV	$\nu \eta'$	958 MeV
$e^\mp K^\pm$	494 MeV	$\nu \phi$	1019 MeV
$\nu \eta$	548 MeV		

Table 3: Relevant final states from HNL (and bino) decay sorted by threshold mass. The active neutrino is considered massless.

⁹ τ leptons are dominantly produced in the decay of the D_s mesons at these experiments.

In Table 4, we list, for each production category, the relevant RPV operator(s) leading to the final states of Table 3. \times indicates that the given final state can not arise for the considered production mode, owing to kinematics. This table can be used to identify all relevant two-coupling RPV scenarios that can be constrained by existing HNL DV searches. Note that we have not included bino production modes corresponding to the $LL\bar{E}$ decays of the τ leptons in the table since these lead to weak limits, as in the one-coupling scenarios. We now discuss numerical results for a representative subset of the possibilities in the table.

4.2.1 Pion scenarios

For the π^\pm category, we consider the two benchmark scenarios listed in Table 5. The relevant mass range is identified by requiring that the production of the neutralino, and its subsequent decay (*cf.* Table 4), should be both kinematically accessible.

We use this opportunity to explain one more subtlety of our recasting procedure for DV searches. In the HNL model, the relevant pion decay process occurs via the neutrino-mixings, *e.g.*, $\pi^\pm \rightarrow e^\pm + N$ via U_e . However, a non-zero U_e also induces the production of the HNL via decays of other particles, *e.g.*, $K^\pm \rightarrow e^\pm + N$ and the three-body decay, $K^\pm \rightarrow e^\pm + \pi^0 + N$. On the other hand, in our RPV benchmarks, this is not the case since λ'_{i11} only couples to the pion. This affects the kinematics of the HNL relative to the bino, and can be an issue for our simple scaling procedure, *cf.* the discussion in Sec. 3. For the pion benchmarks of Table 5, this is not a problem since the kaon modes are sub-dominant ($\mathcal{O}(1\%)$) for the mass range identified above: $1 \text{ MeV} \lesssim m_N \lesssim 139 \text{ MeV}$; see, for instance, Ref. [139] for a plot with the relevant branching ratios in the HNL scenario. However, in later benchmarks, we deal with this issue – if it arises – by restricting the mass range of the benchmark to ensure that the types of contributing parents are the same in both models (neglecting sub-dominant contributions up to $\mathcal{O}(10\%)$), so that the assumption of the same kinematics taken in the DV quick recasting method still holds.

Category	$\tilde{\chi}_1^0$ Production	$\tilde{\chi}_1^0$ Decay	$\nu e e$	$\nu e \mu$	$\nu \mu \mu$	$e\{\pi/\rho\}$	$\mu\{\pi/\rho\}$	eK	μK	$\nu\{\pi/\rho/\omega\}$	$\nu\{\eta/\eta'/\phi\}$
π	$\lambda'_{111} : \pi^\pm \rightarrow e^\pm + \tilde{\chi}_1^0$ ($m_{\tilde{\chi}_1^0} \lesssim 139 \text{ MeV}$) $\lambda'_{211} : \pi^\pm \rightarrow \mu^\pm + \tilde{\chi}_1^0$ ($m_{\tilde{\chi}_1^0} \lesssim 34 \text{ MeV}$)	$\lambda_{121}; \lambda_{131}$ $\lambda_{121}; \lambda_{131}$	$\lambda_{121}; \lambda_{122}; \lambda_{321}; \lambda_{312}$ \times	\times	\times	\times	\times	\times	\times	\times	\times
						λ'_{111}	λ'_{211}	\times	\times	\times	\times
K	$\lambda'_{112} : K^\pm \rightarrow e^\pm + \tilde{\chi}_1^0$ ($m_{\tilde{\chi}_1^0} \lesssim 493 \text{ MeV}$) $\lambda'_{212} : K^\pm \rightarrow \mu^\pm + \tilde{\chi}_1^0$ ($m_{\tilde{\chi}_1^0} \lesssim 388 \text{ MeV}$)	$\lambda_{121}; \lambda_{131}$ $\lambda_{121}; \lambda_{131}$	$\lambda_{121}; \lambda_{122}; \lambda_{321}; \lambda_{312}$ $\lambda_{121}; \lambda_{122}; \lambda_{321}; \lambda_{312}$	$\lambda_{122}; \lambda_{322}$ $\lambda_{122}; \lambda_{322}$	$\lambda_{122}; \lambda_{322}$ $\lambda_{122}; \lambda_{322}$	λ'_{111}	λ'_{211}	\times	\times	λ'_{111}	\times
						λ'_{111}	λ'_{211}	\times	\times	λ'_{111}	\times
D	$\lambda'_{a21} : D^\pm \rightarrow e^\pm + \tilde{\chi}_1^0$ ($m_{\tilde{\chi}_1^0} \leq m_D - m_{e_a}$)	$\lambda_{121}; \lambda_{131}$	$\lambda_{121}; \lambda_{122}; \lambda_{321}; \lambda_{312}$	$\lambda_{122}; \lambda_{322}$	$\lambda_{122}; \lambda_{322}$	λ'_{111}	λ'_{211}	λ'_{112}	λ'_{212}	λ'_{111}	$\lambda'_{111}; \lambda'_{222}$
D_s	$\lambda'_{a22} : D_s^\pm \rightarrow e^\pm + \tilde{\chi}_1^0$ ($m_{\tilde{\chi}_1^0} \leq m_{D_s} - m_{e_a}$)	$\lambda_{121}; \lambda_{131}$	$\lambda_{121}; \lambda_{122}; \lambda_{321}; \lambda_{312}$	$\lambda_{122}; \lambda_{322}$	$\lambda_{122}; \lambda_{322}$	λ'_{111}	λ'_{211}	λ'_{112}	λ'_{212}	λ'_{111}	$\lambda'_{111}; \lambda'_{222}$
B	$\lambda'_{113} : B^\pm(B^0) \rightarrow e_i^\pm(\nu_i) + \tilde{\chi}_1^0$ ($m_{\tilde{\chi}_1^0} \leq m_B - m_{e_i}$)	$\lambda_{121}; \lambda_{131}$	$\lambda_{121}; \lambda_{122}; \lambda_{321}; \lambda_{312}$	$\lambda_{122}; \lambda_{322}$	$\lambda_{122}; \lambda_{322}$	λ'_{111}	λ'_{211}	λ'_{112}	λ'_{212}	λ'_{111}	$\lambda'_{111}; \lambda'_{222}$
B_c	$\lambda'_{223} : B_c^\pm \rightarrow e_i^\pm + \tilde{\chi}_1^0$ ($m_{\tilde{\chi}_1^0} \leq m_{B_c} - m_{e_i}$)	$\lambda_{121}; \lambda_{131}$	$\lambda_{121}; \lambda_{122}; \lambda_{321}; \lambda_{312}$	$\lambda_{122}; \lambda_{322}$	$\lambda_{122}; \lambda_{322}$	λ'_{111}	λ'_{211}	λ'_{112}	λ'_{212}	λ'_{111}	$\lambda'_{111}; \lambda'_{222}$
τ	$\lambda'_{311} : \tau^\pm \rightarrow \{\pi^\pm/\rho^\pm\} + \tilde{\chi}_1^0$ ($m_{\tilde{\chi}_1^0} \lesssim 1637 \text{ MeV}$) $\lambda'_{312} : \tau^\pm \rightarrow K^\pm + \tilde{\chi}_1^0$ ($m_{\tilde{\chi}_1^0} \lesssim 1283 \text{ MeV}$)	$\lambda_{121}; \lambda_{131}$ $\lambda_{121}; \lambda_{131}$	$\lambda_{121}; \lambda_{122}; \lambda_{321}; \lambda_{312}$ $\lambda_{121}; \lambda_{122}; \lambda_{321}; \lambda_{312}$	$\lambda_{122}; \lambda_{322}$ $\lambda_{122}; \lambda_{322}$	$\lambda_{122}; \lambda_{322}$ $\lambda_{122}; \lambda_{322}$	λ'_{111}	λ'_{211}	λ'_{112}	λ'_{212}	λ'_{a11}	$\lambda'_{a11}; \lambda'_{222}$
						λ'_{111}	λ'_{211}	λ'_{112}	λ'_{212}	λ'_{111}	$\lambda'_{111}; \lambda'_{222}$

Table 4: Relevant two-coupling RPV scenarios probed by HNL DV searches. Column one categorizes the parent meson/lepton; column two shows the corresponding RPV coupling, production process, and bino mass range; the remaining columns list the relevant final states of Table 3 arising from bino decays and the corresponding decay RPV coupling(s) for each production category. \times indicates that the decay is kinematically disallowed.

Label	Production	Decay	$m_{\tilde{\chi}_1^0}$
π_1	λ'_{111}	λ_{321}	106 MeV – 139 MeV
π_2	λ'_{211}	λ_{121}	1 MeV – 34 MeV

Table 5: Details of the two-coupling RPV benchmark scenarios we study, corresponding to bino production from pions. The decay coupling in the third column leads to the final state that can be read off from Table 4. See the main text for details on how the mass range is determined.

We show the reinterpreted limits for the benchmarks π_1 and π_2 in the RPV coupling vs. mass plane in Fig. 7a and Fig. 7b, respectively. For two-dimensional visualization, we have set the production and decay couplings to be equal. The exclusion limits come from a corresponding HNL search at Super-Kamiokande [105], as well as projections of sensitivity at DUNE [96]. The former only constrains the mass range $m_N \gtrsim 50$ MeV and, hence, does not have sensitivity to π_2 . We also show the existing bounds on the RPV couplings, taken from Ref. [56]. There are no existing product bounds on the pairs considered [50, 72]. From Fig. 7a, it appears that the existing bound on λ'_{111} outperforms the reinterpreted bound. However, this is an artefact of the choice to set the production and decay couplings equal. We show the same exclusion limits again in Fig. 7c – this time in the coupling vs. coupling plane for a fixed neutralino mass, $m_{\tilde{\chi}_1^0} = 120$ MeV; one can see that the reinterpreted sensitivity projection can probe a small region of the phase space still allowed by the current limits.

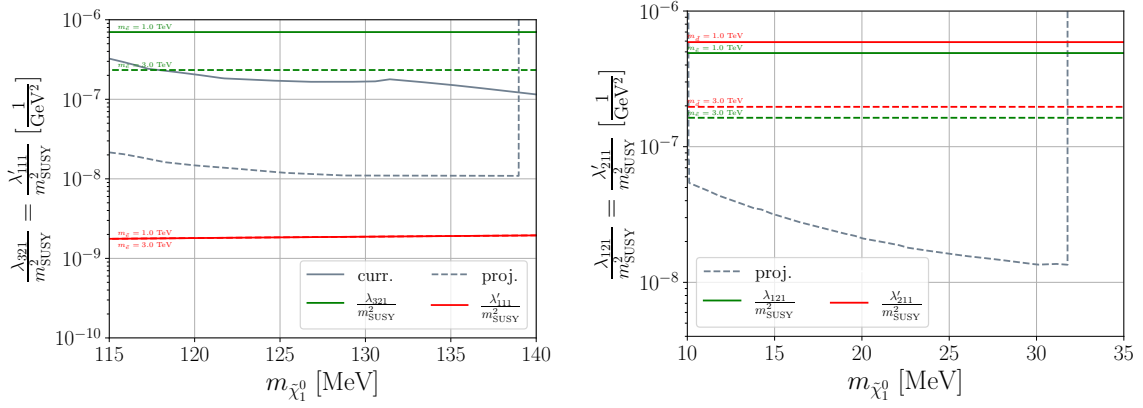
4.2.2 Kaon scenarios

Next, we study benchmarks corresponding to bino production via K^\pm decays; the details are summarized in Table 6. Note, that for some benchmarks, (*e.g.*, \mathbf{K}_3), the lower end of the mass range lies significantly above the kinematic threshold requirement of bino decay. This is, as discussed above, to ensure that kaons are the only parents in the HNL model, as they are in the RPV model.

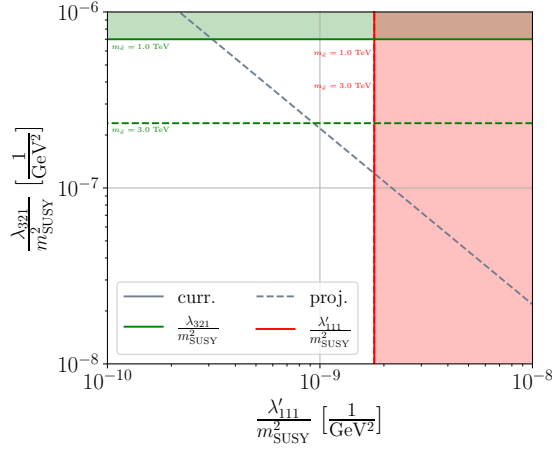
Label	Production	Decay	$m_{\tilde{\chi}_1^0}$
\mathbf{K}_1	λ'_{112}	λ'_{111}	140 MeV – 493 MeV
\mathbf{K}_2	λ'_{112}	λ'_{311}	140 MeV – 493 MeV
\mathbf{K}_3	λ'_{112}	λ_{321}	140 MeV – 493 MeV
\mathbf{K}_4	λ'_{212}	λ'_{211}	140 MeV – 388 MeV
\mathbf{K}_5	λ'_{212}	λ_{131}	35 MeV – 388 MeV

Table 6: As in Table 5 but for bino production from kaons.

The sensitivity limits for the kaon benchmarks are shown in Fig. 8. The single and – wherever relevant – product bounds (taken from Ref. [50, 72]) on RPV couplings are also shown. Current exclusion limits are obtained by combining the results from existing HNL searches at T2K [97], Super-Kamiokande [105], NuTeV [101], and MicroBooNE [102, 140],



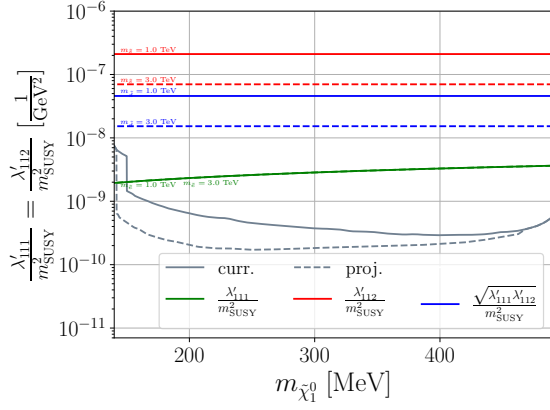
(a) Limits in the RPV coupling vs. bino mass plane for the benchmark π_1 of Table 5. (b) Limits in the RPV coupling vs. bino mass plane for the benchmark π_2 of Table 5.



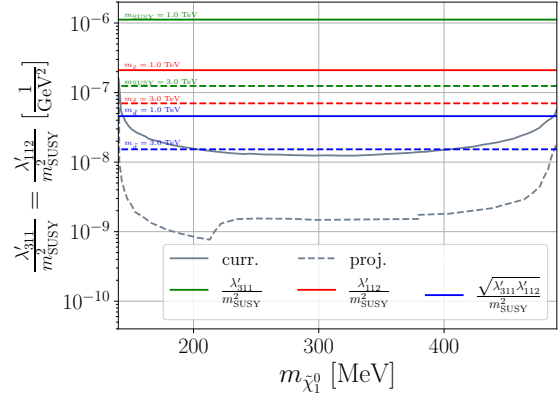
(c) Limits in the production coupling vs. decay coupling plane for the benchmark π_1 of Table 5, with neutralino mass fixed at 120 MeV.

Figure 7: Current exclusion (solid lines) and projected sensitivity (dashed lines) limits corresponding to the two-coupling RPV scenarios with binos produced from pions; reinterpreted from HNL searches. The existing limits on the RPV couplings are shown in red, and green.

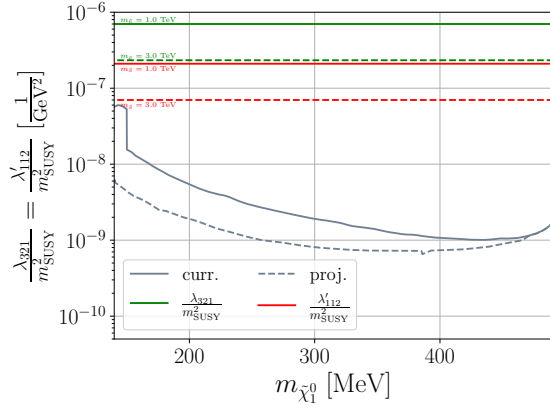
while the projections are all from DUNE [96]. In particular, for the benchmark K_1 , Ref. [141] has studied the sensitivity of Super-Kamiokande to the light binos in the RPV-SUSY, using existing data from the experiment. Their results are found to be comparable with ours. Once again, we see that the reinterpreted limits exclude (or are projected to probe) large swathes of parameter space allowed by the current bounds. The sharp reduction in sensitivity in Fig. 8e below $m_{\tilde{\chi}_1^0} \approx 150 \text{ MeV}$ arises because the most constraining current limit comes from T2K and only probes regions corresponding to $m_N \gtrsim 150 \text{ MeV}$; below this the low-mass searches from Super-K and MicroBooNE provide exclusion.



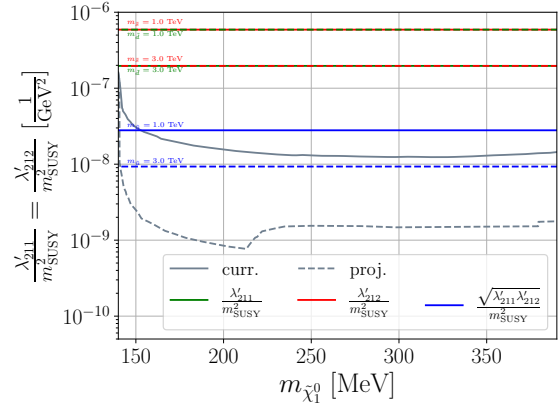
(a) Benchmark K_1 from Table 6.



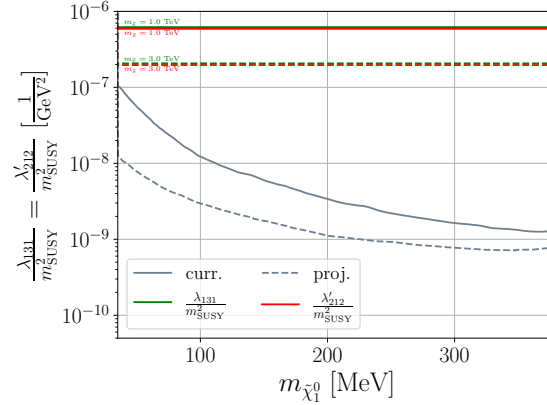
(b) Benchmark K_2 from Table 6.



(c) Benchmark K_3 from Table 6.



(d) Benchmark K_4 from Table 6.



(e) Benchmark K_5 from Table 6.

Figure 8: Current exclusion (solid lines) and projected sensitivity (dashed lines) limits corresponding to the two-coupling RPV scenarios with binos produced from kaons in the RPV coupling vs. bino mass plane; reinterpreted from HNL searches. The existing limits on the RPV couplings are shown in red and green (single bounds), and blue (product bound).

4.2.3 D , D_s , and τ scenarios

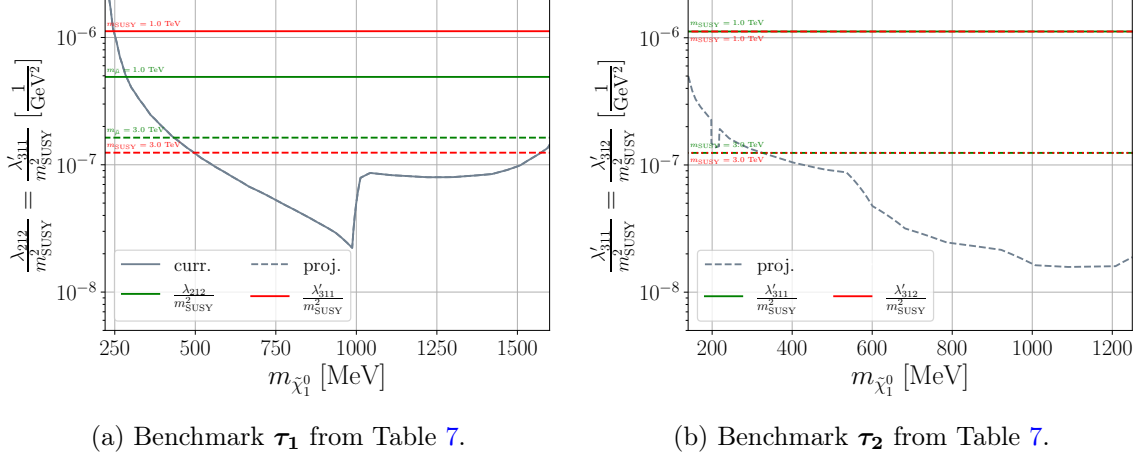


Figure 9: As in Fig. 8 but for binos produced from τ leptons.

We summarize the details for the τ benchmarks we consider, as well as the D^\pm and D_s^\pm meson ones in Table 7. We group them together in this section since, at the considered experiments, τ leptons are most copiously produced in the decays of the D_s mesons. The corresponding sensitivity limits are shown in Fig. 9 for the τ , and in Fig. 10 for the mesons.

Label	Production	Decay	$m_{\tilde{\chi}_1^0}$
τ_1	λ'_{311}	λ_{212}	211 MeV – 1637 MeV
τ_2	λ'_{312}	λ'_{311}	140 MeV – 1283 MeV
D_1	λ'_{122}	λ'_{111}	600 MeV – 1968 MeV
D_2	λ'_{122}	λ'_{211}	600 MeV – 1968 MeV
D_3	λ'_{122}	λ'_{112}	600 MeV – 1968 MeV
D_4	λ'_{122}	λ_{121}	600 MeV – 1968 MeV
D_5	λ'_{222}	λ'_{211}	600 MeV – 1863 MeV
D_6	λ'_{222}	λ_{131}	600 MeV – 1863 MeV
D_7	λ'_{221}	λ_{232}	260 MeV – 1764 MeV

Table 7: As in Table 5 but for bino production from τ leptons, and D and D_s mesons.

For the τ lepton scenarios, the exclusion and projected search sensitivity, shown in Fig. 9, come from BEBC [103, 104], CHARM [98, 142], and ArgoNeUT [143]; and DUNE [96], FASER2 [106, 116], and MoEDAL-MAPP2 [107, 116], respectively. There is no current search targeting the final state of τ_2 , while the current limit on τ_1 beats even the projected search sensitivity at DUNE and FASER. The sharp drop in sensitivity in Fig. 9a at $m_{\tilde{\chi}_1^0} \approx 1000$ MeV occurs because the ρ and bino decay mode of the τ lepton in the RPV model (*cf.* Table 2) becomes kinematically inaccessible, leading to the reduction in production.

For the D and D_s mesons, current exclusions are provided by searches at BEBC [103, 104], CHARM [98], and NuTeV [101]. Further, DUNE [96], FASER2 [106], and MoEDAL-MAPP2 [107, 116] are projected to improve this reach. For all D_s benchmarks except $\mathbf{D_7}$, we only consider neutralinos with mass, $m_{\tilde{\chi}_1^0} > 600$ MeV. This is because either the above experiments only constrain the corresponding parameter region in the HNL model, or because kaons and pions dominate the HNL production for lower masses. One exception is BEBC, where nearly all produced pions and kaons are absorbed by a high-density target before they can decay, and HNL production is dominated by D meson decays. Since benchmark $\mathbf{D_7}$ involves production from D -mesons, we can probe lower bino masses in our scenario. The kink in the corresponding sensitivity limit in Fig. 10g at $m_{\tilde{\chi}_1^0} \approx 500$ MeV occurs because CHARM takes over from BEBC. We note that the final states of benchmarks $\mathbf{D_1}$ and $\mathbf{D_3}$ are not covered by the existing searches but will be covered by the upcoming experiments.

Once again, we see – for all the plots in this section – that reinterpreting existing and projected limits on HNL models in terms of our RPV scenarios gives bounds on the parameter space that improve upon existing limits by orders of magnitude.

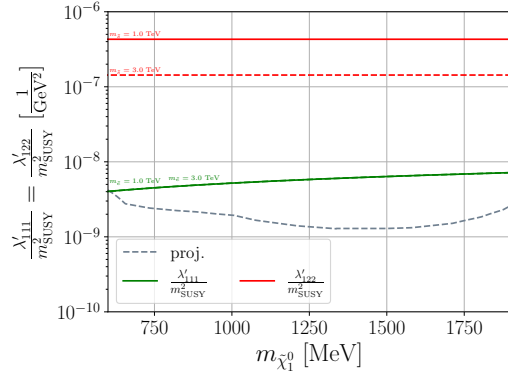
4.2.4 B and B_c scenarios

Here, the bino is produced in $B(B^\pm/B^0)$ or B_c^\pm decays, *cf.* Table 8. While HNL production in these modes only becomes dominant above the D -meson thresholds, the projected search sensitivity for FASER(2) provided in Ref. [106] shows the results separately for the HNLs from B -meson decays and from D -meson and kaon decays, enabling us to choose benchmarks with masses lower than the D thresholds. Up to about $m_N \approx 2700$ MeV, the production is dominated by B decays and we choose the first three benchmarks accordingly. Beyond this, B_c decays also become significant, and for $m_N \gtrsim 3500$ MeV, they become the dominant modes; the last two benchmarks focus on this.

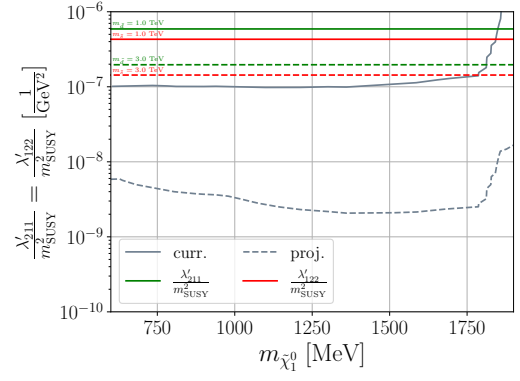
Label	Production	Decay	$m_{\tilde{\chi}_1^0}$
$\mathbf{B_1}$	λ'_{113}	λ'_{122}	548 MeV – 2700 MeV
$\mathbf{B_2}$	λ'_{113}	λ_{131}	160 MeV – 2700 MeV
$\mathbf{B_3}$	λ'_{213}	λ'_{211}	160 MeV – 2700 MeV
$\mathbf{B_4}$	λ'_{123}	λ'_{311}	3500 MeV – 6275 MeV
$\mathbf{B_5}$	λ'_{123}	λ_{131}	3500 MeV – 6275 MeV

Table 8: As in Table 5 but for bino production from B and B_c mesons.

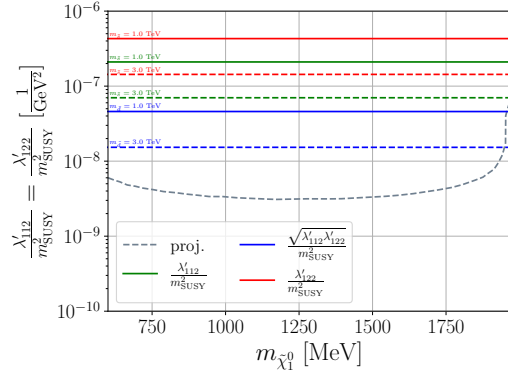
The corresponding sensitivity limits are presented in Fig. 11. There are no existing constraints; however, projections from FASER2 [106, 116] and MoEDAL-MAPP2 [107, 116] show that we should be able to probe the RPV parameter space up to 2-3 orders of magnitude beyond what is ruled out by current limits.



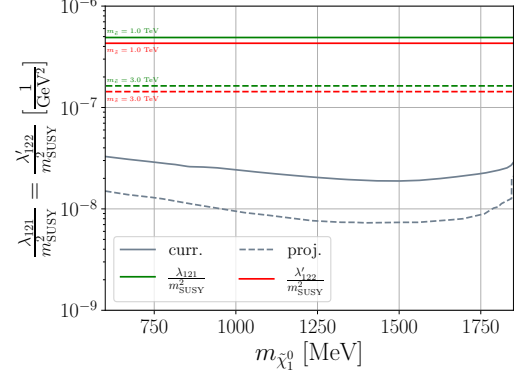
(a) Benchmark D_1 from Table 7.



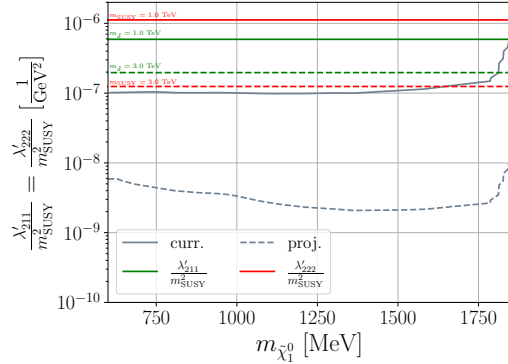
(b) Benchmark D_2 from Table 7.



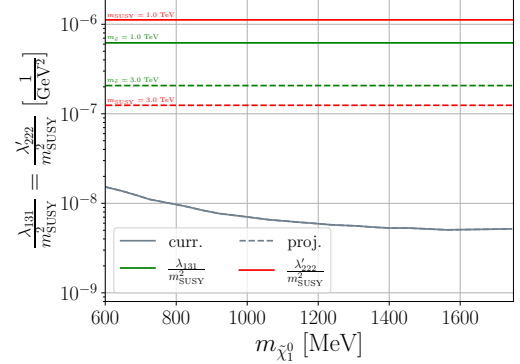
(c) Benchmark D_3 from Table 7.



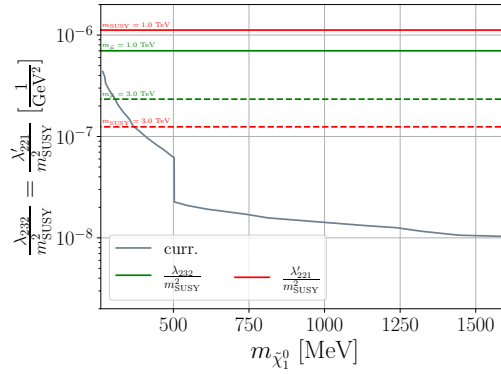
(d) Benchmark D_4 from Table 7.



(e) Benchmark D_5 from Table 7.

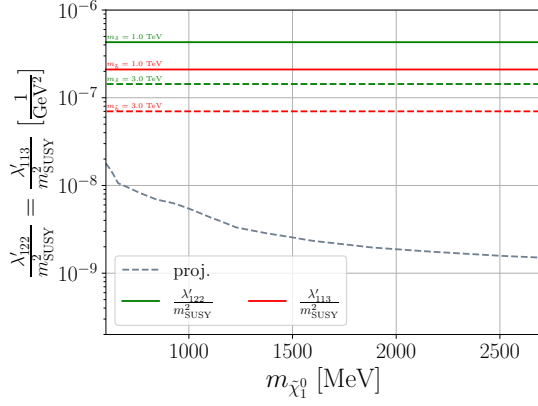


(f) Benchmark D_6 from Table 7.

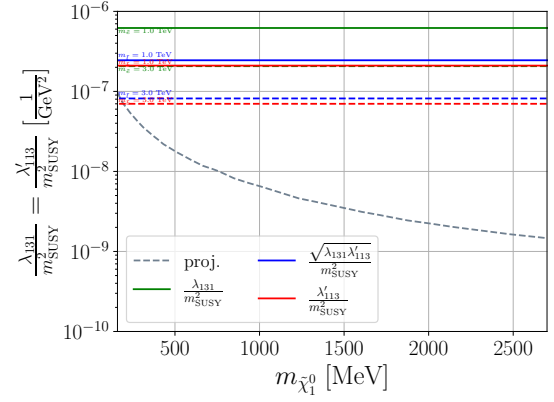


(g) Benchmark D_7 from Table 7.

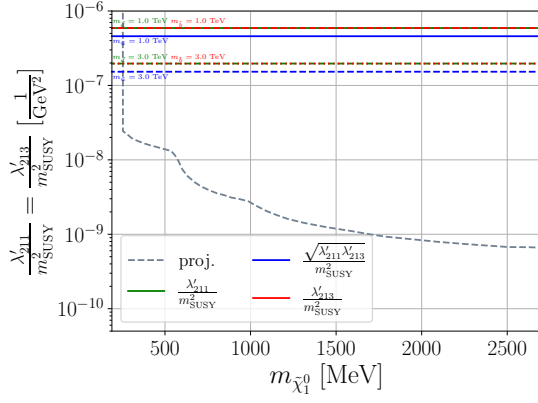
Figure 10: As in Fig. 8 but for bins produced from D and D_s mesons.



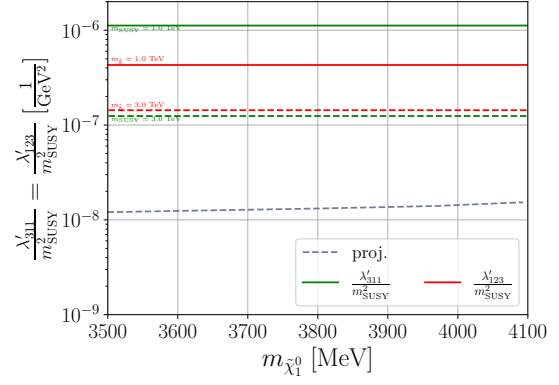
(a) Benchmark $\mathbf{B_1}$ from Table 8.



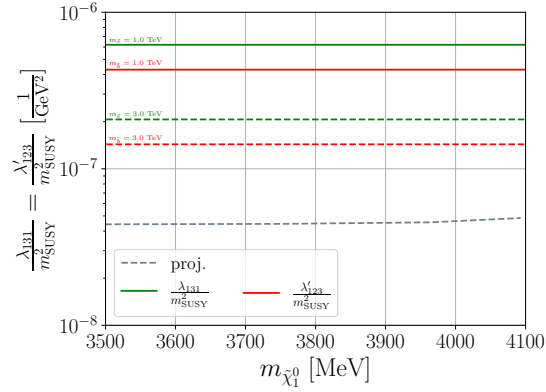
(b) Benchmark $\mathbf{B_2}$ from Table 8.



(c) Benchmark $\mathbf{B_3}$ from Table 8.



(d) Benchmark $\mathbf{B_4}$ from Table 8.



(e) Benchmark $\mathbf{B_5}$ from Table 8.

Figure 11: As in Fig. 8 but for bins produced from B and B_c mesons.

5 Conclusions

In this work, we have considered a GeV-scale or lighter long-lived lightest neutralino, which is necessarily bino-like, in the minimal R-parity-violating (RPV) supersymmetric model. We have focused on lepton-number-violating operators in the RPV superpotential: LH_u , $LL\bar{E}$, and $LQ\bar{D}$. Such light neutralinos are still allowed by all experimental and observational constraints, as long as they decay, for instance via RPV couplings, so as to avoid overclosing the Universe. Since these RPV couplings are bounded to be small, such light binos, which we assume to be the lightest supersymmetric particle in our theory, are expected to have a relatively long lifetime. Via the considered couplings, the binos can decay leptonically or semi-leptonically. For their production, we have focused on rare decays of mesons and charged leptons which are copiously produced at various facilities such as beam-dump and collider experiments. Once produced, these light binos can lead to exotic signatures such as displaced vertices (DVs) or missing energy. We have used searches for these signatures to constrain the RPV couplings associated with a light bino.

These various strategies are experimentally widely utilized to constrain heavy neutral leptons (HNLs) which may decay to almost the same final-state particles as the lightest neutralino in the RPV models. We have thus used the existing HNL searches to set new strict bounds on the relevant RPV couplings. Furthermore we have translated the projected sensitivity to the HNL parameters at certain future experiments into the corresponding search sensitivity for the light neutralinos.

We have studied comprehensively the past experiments PIENU, NA62, T2K, and BaBar, as well as the approved experiments FASER, MoEDAL-MAPP1, PIONEER, and DUNE. We did not consider future experiments that are not yet approved such as MATHUSLA and ANUBIS, with two exceptions, namely FASER2 and MoEDAL-MAPP2 since they would be the follow-up programs of the two currently running experiments FASER and MoEDAL-MAPP1.

Given the various types and flavor-indices of the RPV operators that can be switched on, we have investigated separately different theoretical benchmark scenarios, which can be bounded by distinct experiments and strategies. For the selected representative benchmark scenarios, we have performed numerical computation and presented the final exclusion bounds. Further, we have compared these recast bounds with the existing limits on the RPV couplings which mainly stem from low-energy processes of meson and lepton decays. In general, we find that in most cases the exclusion limits obtained from recasting past HNL searches surpass the existing bounds on the RPV couplings by orders of magnitude, and the expected limits at the considered ongoing and future experiments can be even stronger.

Simple and analytic reinterpretation methods are becoming an important research tool. This is because most published experimental reports present results only for a limited number of simple models, and a recast with full simulation is often complicated and time-consuming. Some existing works such as Refs. [31, 104, 116] have shown the power of simple and quick reinterpretation of searches for long-lived particles by considering heavy neutral leptons in various models and axion-like particles as examples. Our work exemplifies again the strengths and convenience of such reinterpretation methods, by recasting the bounds on the HNLs in the minimal scenario, into those on the lightest neutralinos in the RPV

supersymmetric models, and hence motivates the development of further studies with these reinterpretation methods.

Addendum:

The authors note that Julian Günther et al. are currently working on a dedicated simulation for the same benchmark \mathbf{K}_1 at DUNE in a soon-to-be-released paper.

Acknowledgments

We thank Subir Sarkar and Giacomo Marocco for initial stimulating discussions on their recasting of the BEBC results. We thank Rhorry Gauld for contributions in the early stage of this project, and thank Julian Günther and Martin Hirsch for useful discussions. HKD, DK, SN, and MS acknowledge partial financial support by the Deutsche Forschungsgemeinschaft (DFG, German Research Foundation) through the funds provided to the Sino-German Collaborative Research Center TRR110 “Symmetries and the Emergence of Structure in QCD” (DFG Project ID 196253076 - TRR 110).

A Explicit neutralino production/decay widths with $LL\bar{E}$ operators

In this appendix, we will give the explicit general formulae needed for both the neutralino production and decay via $LL\bar{E}$ couplings at tree level. In the framework of the RPV-MSSM, the relevant processes will always involve four external two-component fermions and one intermediate scalar. The external fermions may carry momenta p_i and have masses m_i , where i is a generic label with $i = 0$ (incoming) and $i = 1, 2, 3$ (outgoing). Following Ref. [85], we express the total decay width as

$$\Gamma_{LL\bar{E}}(0; 1, 2, 3)[\alpha, \beta, \gamma] = \frac{m_0}{2^8 \pi^3} \int_{z_3^{\min}}^{z_3^{\max}} dz_3 \int_{z_1^{\min}}^{z_1^{\max}} dz_1 |\overline{\mathcal{M}}|^2, \quad (\text{A.1})$$

where the spin-averaged matrix element takes the form

$$\begin{aligned} |\overline{\mathcal{M}}|^2 = \frac{m_0^4}{2} & \left[|\alpha|^2 \mathcal{Z}_1 + |\beta|^2 \mathcal{Z}_2 + |\gamma|^2 \mathcal{Z}_3 \right. \\ & - \text{Re} \{ \alpha \beta^* \} \left(+ \mathcal{Z}_1 + \mathcal{Z}_2 - \mathcal{Z}_3 \right) \\ & - \text{Re} \{ \beta \gamma^* \} \left(- \mathcal{Z}_1 + \mathcal{Z}_2 + \mathcal{Z}_3 \right) \\ & \left. - \text{Re} \{ \alpha \gamma^* \} \left(+ \mathcal{Z}_1 - \mathcal{Z}_2 + \mathcal{Z}_3 \right) \right], \quad (\text{A.2}) \end{aligned}$$

with

$$\mathcal{Z}_i \equiv z_i \left(1 - z_i + 2\xi_i^2 - \sum_{j=1}^3 \xi_j^2 \right). \quad (\text{A.3})$$

The kinematic variables z_i are defined as

$$z_i \equiv 2p_0 \cdot p_i / m_0^2 = 2E_i / m_0, \quad (\text{A.4})$$

and fulfill the relation $\sum_{i=1}^3 z_i = 2$. Furthermore we introduce the mass ratios

$$\xi_i \equiv \frac{m_i}{m_0} \quad (i \neq 0). \quad (\text{A.5})$$

The (in general) complex valued coefficients α, β, γ follow from the Feynman rules relevant for the respective process, and can be simplified with the assumption of degenerate sfermion masses, *cf.* Sec. 2. Their explicit expressions are given in Eq. (2.2). The integration limits in Eq. (A.1) can be obtained from the minimal and maximal values of the invariant masses of the “1 – 2” and “2 – 3” systems, *cf.* Ref. [68]:

$$(m_{12}^2)_{\max} = (m_0 - m_3)^2, \quad (\text{A.6})$$

$$(m_{12}^2)_{\min} = (m_1 + m_2)^2, \quad (\text{A.7})$$

$$(m_{23}^2)_{\max} = (E_2^* + E_3^*)^2 - \left(\sqrt{E_2^{*2} - m_2^2} - \sqrt{E_3^{*2} - m_3^2} \right)^2, \quad (\text{A.8})$$

$$(m_{23}^2)_{\min} = (E_2^* + E_3^*)^2 - \left(\sqrt{E_2^{*2} - m_2^2} + \sqrt{E_3^{*2} - m_3^2} \right)^2, \quad (\text{A.9})$$

where the energies $E_{2,3}^*$ in the “1 – 2” rest frame are given in terms of m_{12} by,

$$E_2^* = (m_{12}^2 - m_1^2 + m_2^2) / 2m_{12}, \quad (\text{A.10})$$

$$E_3^* = (m_0^2 - m_{12}^2 - m_3^2) / 2m_{12}. \quad (\text{A.11})$$

From energy-momentum conservation one can deduce that

$$z_3 = \frac{m_0^2 + m_3^2 - m_{12}^2}{m_0^2} \quad \text{and} \quad z_1 = \frac{m_0^2 + m_1^2 - m_{23}^2}{m_0^2}, \quad (\text{A.12})$$

which then finally yield the integration limits:

$$z_3^{\max} = 1 + \xi_3^2 - \frac{(m_{12}^2)_{\min}}{m_0^2}, \quad (\text{A.13})$$

$$z_3^{\min} = 1 + \xi_3^2 - \frac{(m_{12}^2)_{\max}}{m_0^2} = 2\xi_3, \quad (\text{A.14})$$

$$z_1^{\max} = 1 + \xi_1^2 - \frac{(m_{23}^2)_{\min}}{m_{\tilde{\chi}_1^0}^2}, \quad (\text{A.15})$$

$$z_1^{\min} = 1 + \xi_1^2 - \frac{(m_{23}^2)_{\max}}{m_{\tilde{\chi}_1^0}^2}. \quad (\text{A.16})$$

References

- [1] **ATLAS** Collaboration, G. Aad et al., *Observation of a new particle in the search for the Standard Model Higgs boson with the ATLAS detector at the LHC*, *Phys. Lett. B* **716** (2012) 1–29, [[arXiv:1207.7214](#)].
- [2] **CMS** Collaboration, S. Chatrchyan et al., *Observation of a New Boson at a Mass of 125 GeV with the CMS Experiment at the LHC*, *Phys. Lett. B* **716** (2012) 30–61, [[arXiv:1207.7235](#)].
- [3] A. Dedes, H. K. Dreiner, and P. Richardson, *Attempts at explaining the NuTeV observation of dimuon events*, *Phys. Rev. D* **65** (2001) 015001, [[hep-ph/0106199](#)].
- [4] J. L. Feng et al., *Planning the Future of U.S. Particle Physics (Snowmass 2013): Chapter 4: Cosmic Frontier*, in *Snowmass 2013: Snowmass on the Mississippi*, 1, 2014. [[arXiv:1401.6085](#)].
- [5] J. L. Hewett et al., *Planning the Future of U.S. Particle Physics (Snowmass 2013): Chapter 2: Intensity Frontier*, in *Snowmass 2013: Snowmass on the Mississippi*, 1, 2014. [[arXiv:1401.6077](#)].
- [6] J. Alexander et al., *Dark Sectors 2016 Workshop: Community Report*, 8, 2016. [[arXiv:1608.08632](#)].
- [7] M. Battaglieri et al., *US Cosmic Visions: New Ideas in Dark Matter 2017: Community Report*, in *U.S. Cosmic Visions: New Ideas in Dark Matter*, 7, 2017. [[arXiv:1707.04591](#)].
- [8] J. Alimena et al., *Searching for long-lived particles beyond the Standard Model at the Large Hadron Collider*, *J. Phys. G* **47** (2020), no. 9 090501, [[arXiv:1903.04497](#)].
- [9] J. Beacham et al., *Physics Beyond Colliders at CERN: Beyond the Standard Model Working Group Report*, *J. Phys. G* **47** (2020), no. 1 010501, [[arXiv:1901.09966](#)].
- [10] C. A. Argüelles et al., *New opportunities at the next-generation neutrino experiments I: BSM neutrino physics and dark matter*, *Rept. Prog. Phys.* **83** (2020), no. 12 124201, [[arXiv:1907.08311](#)].
- [11] R. K. Ellis et al., *Physics Briefing Book: Input for the European Strategy for Particle Physics Update 2020*, [[arXiv:1910.11775](#)].
- [12] P. Agrawal et al., *Feebly-interacting particles: FIPs 2020 workshop report*, *Eur. Phys. J. C* **81** (2021), no. 11 1015, [[arXiv:2102.12143](#)].
- [13] L. Lee, C. Ohm, A. Soffer, and T.-T. Yu, *Collider Searches for Long-Lived Particles Beyond the Standard Model*, *Prog. Part. Nucl. Phys.* **106** (2019) 210–255, [[arXiv:1810.12602](#)]. [Erratum: *Prog.Part.Nucl.Phys.* 122, 103912 (2022)].
- [14] D. Curtin et al., *Long-Lived Particles at the Energy Frontier: The MATHUSLA Physics Case*, *Rept. Prog. Phys.* **82** (2019), no. 11 116201, [[arXiv:1806.07396](#)].
- [15] S. Knapen and S. Lowette, *A guide to hunting long-lived particles at the LHC*, [[arXiv:2212.03883](#)].
- [16] T. Asaka and M. Shaposhnikov, *The ν MSM, dark matter and baryon asymmetry of the universe*, *Phys. Lett. B* **620** (2005) 17–26, [[hep-ph/0505013](#)].
- [17] P. F. de Salas, D. V. Forero, S. Gariazzo, P. Martínez-Miravé, O. Mena, C. A. Ternes,

- M. Tórtola, and J. W. F. Valle, *2020 global reassessment of the neutrino oscillation picture*, *JHEP* **02** (2021) 071, [[arXiv:2006.11237](#)].
- [18] I. Esteban, M. C. Gonzalez-Garcia, M. Maltoni, T. Schwetz, and A. Zhou, *The fate of hints: updated global analysis of three-flavor neutrino oscillations*, *JHEP* **09** (2020) 178, [[arXiv:2007.14792](#)].
- [19] F. Capozzi, E. Di Valentino, E. Lisi, A. Marrone, A. Melchiorri, and A. Palazzo, *Unfinished fabric of the three neutrino paradigm*, *Phys. Rev. D* **104** (2021), no. 8 083031, [[arXiv:2107.00532](#)].
- [20] P. Minkowski, $\mu \rightarrow e\gamma$ at a Rate of One Out of 10^9 Muon Decays?, *Phys. Lett. B* **67** (1977) 421–428.
- [21] T. Yanagida, *Horizontal gauge symmetry and masses of neutrinos*, *Conf. Proc. C* **7902131** (1979) 95–99.
- [22] M. Gell-Mann, P. Ramond, and R. Slansky, *Complex Spinors and Unified Theories*, *Conf. Proc. C* **790927** (1979) 315–321, [[arXiv:1306.4669](#)].
- [23] R. N. Mohapatra and G. Senjanovic, *Neutrino Mass and Spontaneous Parity Nonconservation*, *Phys. Rev. Lett.* **44** (1980) 912.
- [24] J. Schechter and J. W. F. Valle, *Neutrino Masses in $SU(2) \times U(1)$ Theories*, *Phys. Rev. D* **22** (1980) 2227.
- [25] E. K. Akhmedov, M. Lindner, E. Schnapka, and J. W. F. Valle, *Left-right symmetry breaking in NJL approach*, *Phys. Lett. B* **368** (1996) 270–280, [[hep-ph/9507275](#)].
- [26] E. K. Akhmedov, M. Lindner, E. Schnapka, and J. W. F. Valle, *Dynamical left-right symmetry breaking*, *Phys. Rev. D* **53** (1996) 2752–2780, [[hep-ph/9509255](#)].
- [27] M. Malinsky, J. C. Romao, and J. W. F. Valle, *Novel supersymmetric $SO(10)$ seesaw mechanism*, *Phys. Rev. Lett.* **95** (2005) 161801, [[hep-ph/0506296](#)].
- [28] R. N. Mohapatra and J. W. F. Valle, *Neutrino Mass and Baryon Number Nonconservation in Superstring Models*, *Phys. Rev. D* **34** (1986) 1642.
- [29] M. C. Gonzalez-Garcia and J. W. F. Valle, *Fast Decaying Neutrinos and Observable Flavor Violation in a New Class of Majoron Models*, *Phys. Lett. B* **216** (1989) 360–366.
- [30] HNL, “Heavy Neutrino Limits: <https://github.com/mhostert/Heavy-Neutrino-Limits>.”.
- [31] E. Fernández-Martínez, M. González-López, J. Hernández-García, M. Hostert, and J. López-Pavón, *Effective portals to heavy neutral leptons*, [arXiv:2304.06772](#).
- [32] **ATLAS** Collaboration, G. Aad et al., *Search for long-lived charginos based on a disappearing-track signature using 136 fb^{-1} of pp collisions at $\sqrt{s} = 13\text{ TeV}$ with the ATLAS detector*, *Eur. Phys. J. C* **82** (2022), no. 7 606, [[arXiv:2201.02472](#)].
- [33] **CMS** Collaboration, A. M. Sirunyan et al., *Search for disappearing tracks in proton-proton collisions at $\sqrt{s} = 13\text{ TeV}$* , *Phys. Lett. B* **806** (2020) 135502, [[arXiv:2004.05153](#)].
- [34] D. Choudhury, H. K. Dreiner, P. Richardson, and S. Sarkar, *A Supersymmetric solution to the KARMEN time anomaly*, *Phys. Rev. D* **61** (2000) 095009, [[hep-ph/9911365](#)].
- [35] I. Gogoladze, J. D. Lykken, C. Macesanu, and S. Nandi, *Implications of a Massless Neutralino for Neutrino Physics*, *Phys. Rev. D* **68** (2003) 073004, [[hep-ph/0211391](#)].

- [36] H. K. Dreiner, S. Grab, D. Koschade, M. Kramer, B. O’Leary, and U. Langenfeld, *Rare meson decays into very light neutralinos*, *Phys. Rev. D* **80** (2009) 035018, [[arXiv:0905.2051](#)].
- [37] H. K. Dreiner, S. Heinemeyer, O. Kittel, U. Langenfeld, A. M. Weber, and G. Weiglein, *Mass Bounds on a Very Light Neutralino*, *Eur. Phys. J. C* **62** (2009) 547–572, [[arXiv:0901.3485](#)].
- [38] J. A. Grifols, E. Masso, and S. Peris, *Photinos From Gravitational Collapse*, *Phys. Lett. B* **220** (1989) 591–596.
- [39] J. R. Ellis, K. A. Olive, S. Sarkar, and D. W. Sciama, *Low Mass Photinos and Supernova SN1987A*, *Phys. Lett. B* **215** (1988) 404–410.
- [40] K. Lau, *Constraints on supersymmetry from SN1987A*, *Phys. Rev. D* **47** (1993) 1087–1092.
- [41] H. K. Dreiner, C. Hanhart, U. Langenfeld, and D. R. Phillips, *Supernovae and light neutralinos: SN1987A bounds on supersymmetry revisited*, *Phys. Rev. D* **68** (2003) 055004, [[hep-ph/0304289](#)].
- [42] H. K. Dreiner, M. Kramer, and B. O’Leary, *Bounds on R-parity violating supersymmetric couplings from leptonic and semi-leptonic meson decays*, *Phys. Rev. D* **75** (2007) 114016, [[hep-ph/0612278](#)].
- [43] S. Profumo, *Hunting the lightest lightest neutralinos*, *Phys. Rev. D* **78** (2008) 023507, [[arXiv:0806.2150](#)].
- [44] H. K. Dreiner, M. Hantussek, J. S. Kim, and S. Sarkar, *Gravitino cosmology with a very light neutralino*, *Phys. Rev. D* **85** (2012) 065027, [[arXiv:1111.5715](#)].
- [45] H. K. Dreiner, J.-F. Fortin, J. Isern, and L. Ubaldi, *White Dwarfs constrain Dark Forces*, *Phys. Rev. D* **88** (2013) 043517, [[arXiv:1303.7232](#)].
- [46] D. Hooper and T. Plehn, *Supersymmetric dark matter: How light can the LSP be?*, *Phys. Lett. B* **562** (2003) 18–27, [[hep-ph/0212226](#)].
- [47] L. Calibbi, J. M. Lindert, T. Ota, and Y. Takanishi, *Cornering light Neutralino Dark Matter at the LHC*, *JHEP* **10** (2013) 132, [[arXiv:1307.4119](#)].
- [48] P. Bechtle et al., *Killing the cMSSM softly*, *Eur. Phys. J. C* **76** (2016), no. 2 96, [[arXiv:1508.05951](#)].
- [49] H. K. Dreiner, *An Introduction to explicit R-parity violation*, *Adv. Ser. Direct. High Energy Phys.* **21** (2010) 565–583, [[hep-ph/9707435](#)].
- [50] R. Barbier et al., *R-parity violating supersymmetry*, *Phys. Rept.* **420** (2005) 1–202, [[hep-ph/0406039](#)].
- [51] R. N. Mohapatra, *Supersymmetry and R-parity: an Overview*, *Phys. Scripta* **90** (2015) 088004, [[arXiv:1503.06478](#)].
- [52] F. Domingo and H. K. Dreiner, *Decays of a bino-like particle in the low-mass regime*, [[arXiv:2205.08141](#)].
- [53] B. C. Allanach, A. Dedes, and H. K. Dreiner, *R parity violating minimal supergravity model*, *Phys. Rev. D* **69** (2004) 115002, [[hep-ph/0309196](#)]. [Erratum: *Phys.Rev.D* **72**, 079902 (2005)].
- [54] H. K. Dreiner and G. G. Ross, *R-parity violation at hadron colliders*, *Nucl. Phys. B* **365** (1991) 597–613.

- [55] F. de Campos, O. J. P. Eboli, M. B. Magro, W. Porod, D. Restrepo, M. Hirsch, and J. W. F. Valle, *Probing bilinear R-parity violating supergravity at the LHC*, *JHEP* **05** (2008) 048, [[arXiv:0712.2156](#)].
- [56] D. Dercks, H. Dreiner, M. E. Krauss, T. Opferkuch, and A. Reinert, *R-Parity Violation at the LHC*, *Eur. Phys. J. C* **77** (2017), no. 12 856, [[arXiv:1706.09418](#)].
- [57] H. K. Dreiner, Y. S. Koay, D. Köhler, V. M. Lozano, J. Montejo Berlingen, S. Nangia, and N. Strobbe, *The ABC of RPV: classification of R-parity violating signatures at the LHC for small couplings*, *JHEP* **07** (2023) 215, [[arXiv:2306.07317](#)].
- [58] L. E. Ibanez and G. G. Ross, *Discrete gauge symmetries and the origin of baryon and lepton number conservation in supersymmetric versions of the standard model*, *Nucl. Phys. B* **368** (1992) 3–37.
- [59] H. K. Dreiner, C. Luhn, and M. Thormeier, *What is the discrete gauge symmetry of the MSSM?*, *Phys. Rev. D* **73** (2006) 075007, [[hep-ph/0512163](#)].
- [60] S. Trifinopoulos, *B-physics anomalies: The bridge between R-parity violating supersymmetry and flavored dark matter*, *Phys. Rev. D* **100** (2019), no. 11 115022, [[arXiv:1904.12940](#)].
- [61] Q.-Y. Hu, Y.-D. Yang, and M.-D. Zheng, *Revisiting the B-physics anomalies in R-parity violating MSSM*, *Eur. Phys. J. C* **80** (2020), no. 5 365, [[arXiv:2002.09875](#)].
- [62] Q.-Y. Hu and L.-L. Huang, *Explaining $b \rightarrow s\ell^+\ell^-$ data by sneutrinos in the R-parity violating MSSM*, *Phys. Rev. D* **101** (2020), no. 3 035030, [[arXiv:1912.03676](#)].
- [63] M.-D. Zheng and H.-H. Zhang, *Studying the $b \rightarrow s\ell^+\ell^-$ anomalies and $(g-2)_\mu$ in R-parity violating MSSM framework with the inverse seesaw mechanism*, *Phys. Rev. D* **104** (2021), no. 11 115023, [[arXiv:2105.06954](#)].
- [64] P. S. Bhupal Dev, A. Soni, and F. Xu, *Hints of natural supersymmetry in flavor anomalies?*, *Phys. Rev. D* **106** (2022), no. 1 015014, [[arXiv:2106.15647](#)].
- [65] W. Altmannshofer, P. S. B. Dev, A. Soni, and Y. Sui, *Addressing $R_{D^{(*)}}$, $R_{K^{(*)}}$, muon $g-2$ and ANITA anomalies in a minimal R-parity violating supersymmetric framework*, *Phys. Rev. D* **102** (2020), no. 1 015031, [[arXiv:2002.12910](#)].
- [66] J. H. Collins, P. S. Bhupal Dev, and Y. Sui, *R-parity Violating Supersymmetric Explanation of the Anomalous Events at ANITA*, *Phys. Rev. D* **99** (2019), no. 4 043009, [[arXiv:1810.08479](#)].
- [67] N. Chamoun, F. Domingo, and H. K. Dreiner, *Nucleon decay in the R-parity violating MSSM*, *Phys. Rev. D* **104** (2021), no. 1 015020, [[arXiv:2012.11623](#)].
- [68] **Particle Data Group** Collaboration, R. L. Workman et al., *Review of Particle Physics*, *PTEP* **2022** (2022) 083C01.
- [69] H. K. Dreiner, C. Luhn, H. Murayama, and M. Thormeier, *Baryon triality and neutrino masses from an anomalous flavor $U(1)$* , *Nucl. Phys. B* **774** (2007) 127–167, [[hep-ph/0610026](#)].
- [70] H.-S. Lee, *Minimal gauge origin of baryon triality and flavorful signatures at the LHC*, *Phys. Lett. B* **704** (2011) 316–321, [[arXiv:1007.1040](#)].
- [71] H. K. Dreiner, M. Hanussek, J.-S. Kim, and C. H. Kom, *Neutrino masses and mixings in*

- the baryon triality constrained minimal supersymmetric standard model, *Phys. Rev. D* **84** (2011) 113005, [[arXiv:1106.4338](#)].
- [72] B. C. Allanach, A. Dedes, and H. K. Dreiner, *Bounds on R -parity violating couplings at the weak scale and at the GUT scale*, *Phys. Rev. D* **60** (1999) 075014, [[hep-ph/9906209](#)].
 - [73] P. D. Bolton, F. F. Deppisch, and P. S. B. Dev, *Neutrinoless double beta decay via light neutralinos in R -parity violating supersymmetry*, *JHEP* **03** (2022) 152, [[arXiv:2112.12658](#)].
 - [74] S. Bansal, A. Delgado, C. Kolda, and M. Quiros, *Limits on R -parity-violating couplings from Drell-Yan processes at the LHC*, *Phys. Rev. D* **99** (2019), no. 9 093008, [[arXiv:1812.04232](#)].
 - [75] S. Bansal, A. Delgado, C. Kolda, and M. Quiros, *Constraining R -parity-violating couplings in τ -processes at the LHC and in electroweak precision measurements*, *Phys. Rev. D* **100** (2019), no. 9 093005, [[arXiv:1906.01063](#)].
 - [76] J. L. Pinfold, *The MoEDAL Experiment at the LHC—A Progress Report*, *Universe* **5** (2019), no. 2 47.
 - [77] J. L. Pinfold, *The MoEDAL experiment: a new light on the high-energy frontier*, *Phil. Trans. Roy. Soc. Lond. A* **377** (2019), no. 2161 20190382.
 - [78] **FASER** Collaboration, A. Ariga et al., *FASER’s physics reach for long-lived particles*, *Phys. Rev. D* **99** (2019), no. 9 095011, [[arXiv:1811.12522](#)].
 - [79] J. P. Chou, D. Curtin, and H. J. Lubatti, *New Detectors to Explore the Lifetime Frontier*, *Phys. Lett. B* **767** (2017) 29–36, [[arXiv:1606.06298](#)].
 - [80] **MATHUSLA** Collaboration, C. Alpigiani et al., *An Update to the Letter of Intent for MATHUSLA: Search for Long-Lived Particles at the HL-LHC*, [[arXiv:2009.01693](#)].
 - [81] M. Bauer, O. Brandt, L. Lee, and C. Ohm, *ANUBIS: Proposal to search for long-lived neutral particles in CERN service shafts*, [[arXiv:1909.13022](#)].
 - [82] K. Abe et al., *Letter of Intent: The Hyper-Kamiokande Experiment — Detector Design and Physics Potential* —, [[arXiv:1109.3262](#)].
 - [83] **Hyper-Kamiokande Working Group** Collaboration, E. Kearns et al., *Hyper-Kamiokande Physics Opportunities*, in *Snowmass 2013: Snowmass on the Mississippi*, 9, 2013. [[arXiv:1309.0184](#)].
 - [84] L. J. Hall and M. Suzuki, *Explicit R -Parity Breaking in Supersymmetric Models*, *Nucl. Phys. B* **231** (1984) 419–444.
 - [85] H. K. Dreiner, H. E. Haber, and S. P. Martin, *Two-component spinor techniques and Feynman rules for quantum field theory and supersymmetry*, *Phys. Rept.* **494** (2010) 1–196, [[arXiv:0812.1594](#)].
 - [86] J. de Vries, H. K. Dreiner, and D. Schmeier, *R -Parity Violation and Light Neutralinos at SHiP and the LHC*, *Phys. Rev. D* **94** (2016), no. 3 035006, [[arXiv:1511.07436](#)].
 - [87] H. K. Dreiner, D. Köhler, S. Nangia, and Z. S. Wang, *Searching for a single photon from lightest neutralino decays in R -parity-violating supersymmetry at FASER*, *JHEP* **02** (2023) 120, [[arXiv:2207.05100](#)].
 - [88] M. A. Diaz, *Bilinear R -parity violation*, in *International Workshop on Physics Beyond the Standard Model: From Theory to Experiment (Valencia 97)*, pp. 188–199, 2, 1998. [[hep-ph/9802407](#)].

- [89] **PIENU** Collaboration, A. Aguilar-Arevalo et al., *Improved search for heavy neutrinos in the decay $\pi \rightarrow e\nu$* , *Phys. Rev. D* **97** (2018), no. 7 072012, [[arXiv:1712.03275](#)].
- [90] **PIONEER** Collaboration, W. Altmannshofer et al., *Testing Lepton Flavor Universality and CKM Unitarity with Rare Pion Decays in the PIONEER experiment*, in *Snowmass 2021*, 3, 2022. [[arXiv:2203.05505](#)].
- [91] M. Daum, B. Jost, R. M. Marshall, R. C. Minehart, W. A. Stephens, and K. O. H. Ziock, *Search for Admixtures of Massive Neutrinos in the Decay $\pi^+ \rightarrow \mu^+$ Neutrino*, *Phys. Rev. D* **36** (1987) 2624.
- [92] **NA62** Collaboration, E. Cortina Gil et al., *Search for heavy neutral lepton production in K^+ decays to positrons*, *Phys. Lett. B* **807** (2020) 135599, [[arXiv:2005.09575](#)].
- [93] **NA62** Collaboration, E. Cortina Gil et al., *Search for K^+ decays to a muon and invisible particles*, *Phys. Lett. B* **816** (2021) 136259, [[arXiv:2101.12304](#)].
- [94] Y. Asano et al., *Search for a Heavy Neutrino Emitted in $K^+ \rightarrow \mu^+$ Neutrino Decay*, *Phys. Lett. B* **104** (1981) 84–88.
- [95] R. S. Hayano et al., *HEAVY NEUTRINO SEARCH USING $K(\mu 2)$ DECAY*, *Phys. Rev. Lett.* **49** (1982) 1305.
- [96] P. Ballett, T. Boschi, and S. Pascoli, *Heavy Neutral Leptons from low-scale seesaws at the DUNE Near Detector*, *JHEP* **03** (2020) 111, [[arXiv:1905.00284](#)].
- [97] **T2K** Collaboration, K. Abe et al., *Search for heavy neutrinos with the T2K near detector ND280*, *Phys. Rev. D* **100** (2019), no. 5 052006, [[arXiv:1902.07598](#)].
- [98] **CHARM** Collaboration, F. Bergsma et al., *A Search for Decays of Heavy Neutrinos in the Mass Range 0.5-GeV to 2.8-GeV*, *Phys. Lett. B* **166** (1986) 473–478.
- [99] **CHARM II** Collaboration, P. Vilain et al., *Search for heavy isosinglet neutrinos*, *Phys. Lett. B* **343** (1995) 453–458.
- [100] J. Orloff, A. N. Rozanov, and C. Santoni, *Limits on the mixing of tau neutrino to heavy neutrinos*, *Phys. Lett. B* **550** (2002) 8–15, [[hep-ph/0208075](#)].
- [101] **NuTeV, E815** Collaboration, A. Vaitaitis et al., *Search for neutral heavy leptons in a high-energy neutrino beam*, *Phys. Rev. Lett.* **83** (1999) 4943–4946, [[hep-ex/9908011](#)].
- [102] K. J. Kelly and P. A. N. Machado, *MicroBooNE experiment, NuMI absorber, and heavy neutral leptons*, *Phys. Rev. D* **104** (2021), no. 5 055015, [[arXiv:2106.06548](#)].
- [103] **WA66** Collaboration, A. M. Cooper-Sarkar et al., *Search for Heavy Neutrino Decays in the BEBC Beam Dump Experiment*, *Phys. Lett. B* **160** (1985) 207–211.
- [104] R. Barouki, G. Marocco, and S. Sarkar, *Blast from the past II: Constraints on heavy neutral leptons from the BEBC WA66 beam dump experiment*, *SciPost Phys.* **13** (2022) 118, [[arXiv:2208.00416](#)].
- [105] P. Coloma, P. Hernández, V. Muñoz, and I. M. Shoemaker, *New constraints on Heavy Neutral Leptons from Super-Kamiokande data*, *Eur. Phys. J. C* **80** (2020), no. 3 235, [[arXiv:1911.09129](#)].
- [106] F. Kling and S. Trojanowski, *Heavy Neutral Leptons at FASER*, *Phys. Rev. D* **97** (2018), no. 9 095016, [[arXiv:1801.08947](#)].
- [107] J. De Vries, H. K. Dreiner, J. Y. Günther, Z. S. Wang, and G. Zhou, *Long-lived Sterile Neutrinos at the LHC in Effective Field Theory*, *JHEP* **03** (2021) 148, [[arXiv:2010.07305](#)].

- [108] **BaBar** Collaboration, J. P. Lees et al., *Search for heavy neutral leptons using tau lepton decays at BaBar*, *Phys. Rev. D* **107** (2023), no. 5 052009, [[arXiv:2207.09575](#)].
- [109] **NA62** Collaboration, E. Cortina Gil et al., *Search for π^0 decays to invisible particles*, *JHEP* **02** (2021) 201, [[arXiv:2010.07644](#)].
- [110] **BaBar** Collaboration, J. P. Lees et al., *Improved Limits on B^0 Decays to Invisible Final States and to $\nu\bar{\nu}\gamma$* , *Phys. Rev. D* **86** (2012) 051105, [[arXiv:1206.2543](#)].
- [111] **PIENU** Collaboration, A. Aguilar-Arevalo et al., *Search for heavy neutrinos in $\pi \rightarrow \mu\nu$ decay*, *Phys. Lett. B* **798** (2019) 134980, [[arXiv:1904.03269](#)].
- [112] **PiENu** Collaboration, A. Aguilar-Arevalo et al., *Improved Measurement of the $\pi \rightarrow e\nu$ Branching Ratio*, *Phys. Rev. Lett.* **115** (2015), no. 7 071801, [[arXiv:1506.05845](#)].
- [113] **DUNE** Collaboration, B. Abi et al., *Deep Underground Neutrino Experiment (DUNE), Far Detector Technical Design Report, Volume I Introduction to DUNE*, *JINST* **15** (2020), no. 08 T08008, [[arXiv:2002.02967](#)].
- [114] G. Marocco and S. Sarkar, *Blast from the past: Constraints on the dark sector from the BEBC WA66 beam dump experiment*, *SciPost Phys.* **10** (2021), no. 2 043, [[arXiv:2011.08153](#)].
- [115] J. L. Feng, I. Galon, F. Kling, and S. Trojanowski, *ForwArd Search ExpeRiment at the LHC*, *Phys. Rev. D* **97** (2018), no. 3 035001, [[arXiv:1708.09389](#)].
- [116] R. Beltrán, G. Cottin, M. Hirsch, A. Titov, and Z. S. Wang, *Reinterpretation of searches for long-lived particles from meson decays*, *JHEP* **05** (2023) 031, [[arXiv:2302.03216](#)].
- [117] V. V. Gligorov, S. Knapen, M. Papucci, and D. J. Robinson, *Searching for Long-lived Particles: A Compact Detector for Exotics at LHCb*, *Phys. Rev. D* **97** (2018), no. 1 015023, [[arXiv:1708.09395](#)].
- [118] S. Cerci et al., *FACET: A new long-lived particle detector in the very forward region of the CMS experiment*, *JHEP* **2022** (2022), no. 06 110, [[arXiv:2201.00019](#)].
- [119] D. Dercks, J. De Vries, H. K. Dreiner, and Z. S. Wang, *R-parity Violation and Light Neutralinos at CODEX-b, FASER, and MATHUSLA*, *Phys. Rev. D* **99** (2019), no. 5 055039, [[arXiv:1810.03617](#)].
- [120] D. Dercks, H. K. Dreiner, M. Hirsch, and Z. S. Wang, *Long-Lived Fermions at AL3X*, *Phys. Rev. D* **99** (2019), no. 5 055020, [[arXiv:1811.01995](#)].
- [121] H. K. Dreiner, J. Y. Günther, and Z. S. Wang, *R-parity violation and light neutralinos at ANUBIS and MAPP*, *Phys. Rev. D* **103** (2021), no. 7 075013, [[arXiv:2008.07539](#)].
- [122] **MEG** Collaboration, A. M. Baldini et al., *Search for the lepton flavour violating decay $\mu^+ \rightarrow e^+\gamma$ with the full dataset of the MEG experiment*, *Eur. Phys. J. C* **76** (2016), no. 8 434, [[arXiv:1605.05081](#)].
- [123] D. I. Britton et al., *Improved search for massive neutrinos in $\pi^+ \rightarrow e^+ \text{ neutrino}$ decay*, *Phys. Rev. D* **46** (1992) R885–R887.
- [124] **Borexino** Collaboration, G. Bellini et al., *New limits on heavy sterile neutrino mixing in B_8 decay obtained with the Borexino detector*, *Phys. Rev. D* **88** (2013), no. 7 072010, [[arXiv:1311.5347](#)].
- [125] R. Plestid, *Luminous solar neutrinos II: Mass-mixing portals*, *Phys. Rev. D* **104** (2021)

- 075028, [[arXiv:2010.09523](#)]. [Erratum: Phys.Rev.D 105, 099901 (2022), Erratum: Phys.Rev.D 105, 099901 (2022)].
- [126] M. Dentler, A. Hernández-Cabezudo, J. Kopp, P. A. N. Machado, M. Maltoni, I. Martinez-Soler, and T. Schwetz, *Updated Global Analysis of Neutrino Oscillations in the Presence of eV -Scale Sterile Neutrinos*, *JHEP* **08** (2018) 010, [[arXiv:1803.10661](#)].
 - [127] D. Gorbunov and M. Shaposhnikov, *How to find neutral leptons of the ν MSM?*, *JHEP* **10** (2007) 015, [[arXiv:0705.1729](#)]. [Erratum: JHEP 11, 101 (2013)].
 - [128] D. Gorbunov, I. Krasnov, Y. Kudenko, and S. Suvorov, *Heavy Neutral Leptons from kaon decays in the SHiP experiment*, *Phys. Lett. B* **810** (2020) 135817, [[arXiv:2004.07974](#)].
 - [129] R. E. Shrock, *General Theory of Weak Leptonic and Semileptonic Decays. 1. Leptonic Pseudoscalar Meson Decays, with Associated Tests For, and Bounds on, Neutrino Masses and Lepton Mixing*, *Phys. Rev. D* **24** (1981) 1232.
 - [130] K. Bondarenko, A. Boyarsky, D. Gorbunov, and O. Ruchayskiy, *Phenomenology of GeV-scale Heavy Neutral Leptons*, *JHEP* **11** (2018) 032, [[arXiv:1805.08567](#)].
 - [131] A. S. Joshipura and M. Nowakowski, *'Just so' oscillations in supersymmetric standard model*, *Phys. Rev. D* **51** (1995) 2421–2427, [[hep-ph/9408224](#)].
 - [132] M. Nowakowski and A. Pilaftsis, *W and Z boson interactions in supersymmetric models with explicit R-parity violation*, *Nucl. Phys. B* **461** (1996) 19–49, [[hep-ph/9508271](#)].
 - [133] T. Banks, Y. Grossman, E. Nardi, and Y. Nir, *Supersymmetry without R-parity and without lepton number*, *Phys. Rev. D* **52** (1995) 5319–5325, [[hep-ph/9505248](#)].
 - [134] C. A. Argüelles, N. Foppiani, and M. Hostert, *Heavy neutral leptons below the kaon mass at hodoscopic neutrino detectors*, *Phys. Rev. D* **105** (2022), no. 9 095006, [[arXiv:2109.03831](#)].
 - [135] S. Dey, C. O. Dib, J. Carlos Helo, M. Nayak, N. A. Neill, A. Soffer, and Z. S. Wang, *Long-lived light neutralinos at Belle II*, *JHEP* **02** (2021) 211, [[arXiv:2012.00438](#)].
 - [136] **Belle-II** Collaboration, T. Abe et al., *Belle II Technical Design Report*, [[arXiv:1011.0352](#)].
 - [137] **Belle-II** Collaboration, W. Altmannshofer et al., *The Belle II Physics Book*, *PTEP* **2019** (2019), no. 12 123C01, [[arXiv:1808.10567](#)]. [Erratum: PTEP 2020, 029201 (2020)].
 - [138] M. Hirsch and J. W. F. Valle, *Neutrinoless double beta decay in supersymmetry with bilinear R parity breaking*, *Nucl. Phys. B* **557** (1999) 60–78, [[hep-ph/9812463](#)].
 - [139] J. M. Berryman, A. de Gouvea, P. J. Fox, B. J. Kayser, K. J. Kelly, and J. L. Raaf, *Searches for Decays of New Particles in the DUNE Multi-Purpose Near Detector*, *JHEP* **02** (2020) 174, [[arXiv:1912.07622](#)].
 - [140] **MicroBooNE** Collaboration, P. Abratenko et al., *Search for long-lived heavy neutral leptons and Higgs portal scalars decaying in the MicroBooNE detector*, *Phys. Rev. D* **106** (2022), no. 9 092006, [[arXiv:2207.03840](#)].
 - [141] P. Candia, G. Cottin, A. Méndez, and V. Muñoz, *Searching for light long-lived neutralinos at Super-Kamiokande*, *Phys. Rev. D* **104** (2021), no. 5 055024, [[arXiv:2107.02804](#)].
 - [142] I. Boiarska, A. Boyarsky, O. Mikulenko, and M. Ovchinnikov, *Constraints from the CHARM experiment on heavy neutral leptons with tau mixing*, *Phys. Rev. D* **104** (2021), no. 9 095019, [[arXiv:2107.14685](#)].

- [143] **ArgoNeuT** Collaboration, R. Acciarri et al., *New Constraints on Tau-Coupled Heavy Neutral Leptons with Masses $m_N=280-970$ MeV*, *Phys. Rev. Lett.* **127** (2021), no. 12 121801, [[arXiv:2106.13684](#)].